Titre: Title:	Effect of Saccade on Spatial Localization in the Macaque Primate Cortical Area V4
Auteur: Author:	Taban Akbarzadeh Shafarudi
Date:	2021
Type:	Mémoire ou thèse / Dissertation or Thesis
Référence: Citation:	Akbarzadeh Shafarudi, T. (2021). Effect of Saccade on Spatial Localization in the Macaque Primate Cortical Area V4 [Master's thesis, Polytechnique Montréal]. PolyPublie. https://publications.polymtl.ca/6327/

Document en libre accès dans PolyPublie
Open Access document in PolyPublie

URL de PolyPublie: PolyPublie URL:	https://publications.polymtl.ca/6327/
Directeurs de recherche: Advisors:	Frédéric Lesage, & Mohamad Sawan
Programme: Program:	Génie électrique

POLYTECHNIQUE MONTRÉAL

affiliée à l'Université de Montréal

Effect of saccade on spatial localization in the macaque primate cortical area V4

TABAN AKBARZADEH SHAFARUDI

Département de Génie électrique

Mémoire présenté en vue de l'obtention du diplôme de *Maîtrise ès sciences appliquées*
Génie électrique

Avril 2021

POLYTECHNIQUE MONTRÉAL

affiliée à l'Université de Montréal

Ce mémoire intitulé :

Effect of saccade on spatial localization in the macaque primate cortical area V4

présenté par **Taban AKBARZADEH SHAFARUDI**
en vue de l'obtention du diplôme de *Maîtrise ès sciences appliquées*
a été dûment accepté par le jury d'examen constitué de :

Richard GOURDEAU, président
Frédéric LESAGE, membre et directeur de recherche
Mohamad SAWAN, membre et codirecteur de recherche
Frédéric LEBLOND, membre

DEDICATION

To my beloved parents

ACKNOWLEDGEMENTS

RÉSUMÉ

La stimulation de diverses parties du flux de traitement visuel, comme le cortex visuel primaire, est devenue l'un des défis les plus captivants de l'étude de la vision artificielle. Cependant, fournir un percept artificiel comparable à la vision naturelle est difficile en raison de la complexité du système visuel. L'un des défis majeurs des prothèses visuelles est de concevoir des dispositifs capables d'interagir efficacement avec le cortex visuel. Malgré la recherche en microsimulation visuelle, il existe un constat d'échec de ces dispositifs à mettre à jour les informations visuelles pendant les mouvements oculaires pour visualiser l'environnement. Cette faiblesse nuit à la création d'un percept similaire au système visuel naturel. De plus, les dispositifs prosthétiques visuels nécessitent une stratégie de pondération d'électrode pour générer un motif de microstimulation électrique à une position spécifique. Ces poids pour chaque électrode sont déterminés par un décodeur qui discrimine les positions. Dans des applications réelles, en présence de mouvements oculaires saccadiques, générer une perception stable nécessite une imitation des phénomènes de suppression saccadique et de déplacement sur les poids d'électrodes. Dans ce travail, nous nous concentrons sur l'effet du déplacement sur les poids de décodage attribués aux électrodes lors de la localisation en proposant un décodeur capable de décoder une position aussi précise que le système visuel réel même lors des mouvements oculaires, à l'aide d'un apprentissage automatique supervisé.

ABSTRACT

In recent years, stimulating various parts of the visual processing stream, such as the primary visual cortex, has become one of the most captivating challenges in artificial vision studies. However, providing an artificial percept comparable with natural vision is significantly difficult due to the complexity of the visual system. One of the major challenges in visual prostheses is to design devices with the ability to effectively interact with the visual brain. Despite all assessments in visual microsimulation, there are reports regarding the failure of these devices in updating visual information during eye movements for interfacing the environment. This weakness makes difficult the creation of a percept that is similar to the natural visual system. Visual prosthetic devices need an electrode weighting strategy to generate an electrical microstimulation pattern at specific positions. These weights for each electrode are determined by a decoder that discriminates positions. In real applications, in presence of saccadic eye movements, generating a stable percept require imitation of the saccadic suppression and remapping phenomena on electrode weights. In this work, we focus on the effect of remapping on the decoding weights assigned to the electrodes during localization by proposing a decoder which is able to decode position as precise as the real visual system even during eye movements, with the assist of a supervised machine learning algorithm.

TABLE OF CONTENTS

LIST OF TABLES

LIST OF FIGURES

LIST OF SYMBOLS AND ACRONYMS

FF   Future Field

CF   Current Field

ST   Saccade Target

RF   Receptive Field

WF   Weight Field

V1   Visual area V1

V4   Visual area V4

LIP   Lateral Intraparietal area

LFP   Local Field Potential

MUA   Multiunit Activity

SVM   Support Vector Machine

CHAPTER 1   INTRODUCTION

In recent years, stimulating various parts of the visual processing stream, such as the primary visual cortex, has become one of the most captivating challenges in artificial vision studies. However, providing an artificial percept comparable with natural vision is significantly difficult due to the complexity of the visual system [4–6]. One of the major challenges in visual prostheses is to design devices with the ability to effectively interact with the visual brain. Despite all assessments in visual microsimulation, there are reports regarding the failure of these devices in updating visual information during eye movements when perceiving the environment [4]. This weakness limits the creation of a percept that is similar to the natural visual system.

One of the main and significant movement in humans is eye movement. We move our eyes to investigate the world around. By these movements, the location of an object changes in retinal space [4,5,7,8]. However, even with this displacement, the visual system provides us a stable percept of the world due to brain compensation. Consequently, we do not see a shaky world. Saccadic suppression is one of the brain compensation mechanism which helps in providing a stable perception of our surroundings [9]. In a normal visual system, the brain decreases neural responses around the time of each eye movement such that humans do not perceive these movements. This phenomenon is referred as saccadic suppression. Thus, to have an artificial percept similar to the natural visual system, the visual prostheses devices need to provide such a mechanism in order to make perception continuous. Though current studies give us optimistic pictures about artificial vision, still there are unanswered questions. In particular, to provide a saccadic suppression mechanism, by means of electrical stimulation, in order to deliver a continuous perception of the world for the lifetime of blind people is still a major challenge. On the other hand, Goldberg *et al.* 1992 [10] showed that remapping is the visual system solution for the retinal displacement during saccade. However, this remapping causes a transient shift of neuron's receptive field from presaccadic to postsaccadic spatial locations, but it has a functional role in providing stable perception [3,10].

To generate an electrical microstimulation pattern, visual prosthetic devices need a weight field strategy to generate a phosphene (cortical representation of light points) at specific position. The weight of each electrode is determined by a decoder that discriminates positions [11]. However, in real applications, when eye movement is involved, generating a stable

percent require imitation of the saccadic suppression [12] and remapping [3, 10] phenomena on weight fields. In this work, we focus on the effect of remapping on the decoding weights assigned to the electrodes during localization.

1.1 Eye movement and visual perception

Vision is the primary method for people to receive information from their environment. Unfortunately, visual impairment has a devastating impact on the quality of life of millions of people around the world and raises for them extraordinary difficulties in a society that is highly reliant on sight.

In order to enhance the quality of life of blind people, numerous studies on artificial vision have been conducted. These have raised expectations that retinal implants and other vision-restoration approaches will be developed for blind individuals. Fortunately, such researches could develop visual prostheses in the form of visual implants. The implantable electronic device is known as a visual prosthesis or artificial vision. Electronic visual prostheses have been proposed as a means to restore a basic sense of sight to people with profound vision loss [13]. In other words, they aim to recover partial vision in blind patients with the assist of stimulating the retinal cells, optic nerve, or visual cortex [14]. A significant problem for the creation of cortical visual prostheses is to identify the cortical representation of light points, known as phosphenes, by assigning correct stimulation parameters to implanted electrodes.

When we try to move our eye-ball with a finger, we can experience the distorted image in our percept. Like a filmmaker who ensures an intricate combination of camera's tripod, lighting, focus and stability to capture events after discovering the ideal panorama to capture in his camera, minor movements in any of these components can wreck the footage. On the other hand, our perception from the visual world stays persistent despite numerous eye movements we make continuously to see the world and objects. Although technology has enabled us to build extremely stable instruments that record steady videos, nature has created its way of allowing stable visual perception with large and small eye movements. The visual system helps us not only in seeing but also to search, analyse, understand and then decide. In fact, the analogy would not be equitable between the visual system and a camera with limited purposes. However, this analogy helps us to put things in perspective and raises the intriguing question of how the brain is providing us a stable percept of the world despite the movements

in the retina. This is one of the challenges in the reproduction of an artificial vision very similar to the human visual system.

Each second, we make about three abrupt eye movements called *saccade* in order to scan the world around us. As we move our eyes, a fixed object excites consecutive locations on the retina [10]. However, despite this shifted input, we discern a clear stable vision. In other words, as a consequence of saccadic eye movements, objects in the world have various positions on the retina from one fixation (the still periods between *saccade*) to another. Saccadic eye movement schematic was illustrated in 1.1.

Our eyes jump from word to word while reading this text. However, that we are not aware of the motion in our retina, thanks to our brain which compensates for these replacements to provide us a stable percept of the world. However, this compensation is not ideal and perisaccadically perceptual space is distorted [15]. In this thesis, it is shown that this distortion can be traced to a representation of the retinal position in visual area V4 and consequently to the localization of phosphenes in order to provide blind people meaningful percept like what pictures in figure 1.1, by means of the prosthesis.

1.2 Electrical simulation

Visual prostheses are used to restore the vision function of blind people by reconstructing their ability to recognize objects and navigate in an unfamiliar environment [16]. Since blindness is due to impairment of natural visual signal transmission, optical prostheses are often used to activate the visual pathways at certain still functioning locations beyond the affected site [17].

Using the electrical current stimulation of the optical cortex at specific locations evokes the illusion of phosphenes, which are illuminated, isolated, and spatially located light spots near to the centre of the field of vision. Electrical stimulation of the visual path through multi-electrode arrays provides the ability to inject a spatiotemporal activity pattern in order to induce a path of phosphenic perception to evoke visual percepts as a phosphened visual scene [2, 5, 16, 18–21]. Various areas can be activated by electrical stimulation, for instance, the retina, optic nerve and visual cortex, depending on the damaged visual pathway. In
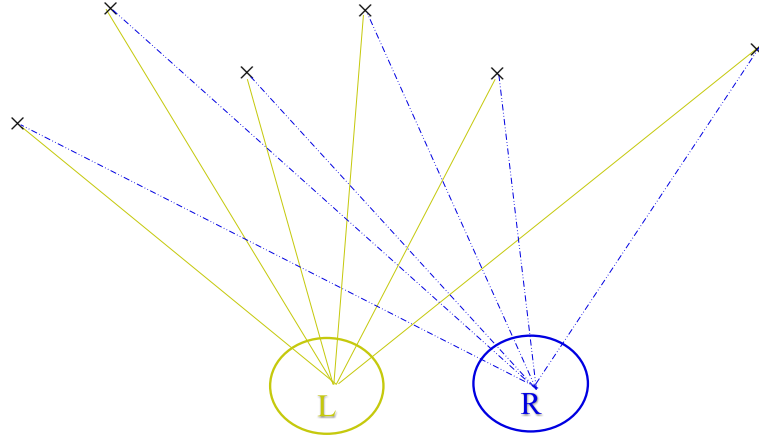
Figure 1.1 **Schematic of saccadic eye movement.** Saccade is a fast eye moment that allows scanning the visual scene in order to have a stable percept. Eyes fix on each position for a short time before jumping to the next position. Basically, for example, while reading our eyes are focusing on areas a bit apart from a specific character. This shows that saccade carries out the information from the next position that helps to do not have discrete images. Blue and green circles are showing right and left eyeballs respectively. Crosses are showing examples of fixation and target positions for saccade.

people with normal sight, the retina carries out spatial, temporal and chromatic processing on visual input. In addition, it generates sequences of spikes transferred to Lateral Geniculate Nucleus (LGN), then projected to the cortex visual area V1 and, finally, to areas, V2, V3, V4, and V5, figure 2.2.

Visual area V1 is an adequate site for implanting electrode arrays since it has a uniform thickness, a high density of cells for central vision, and visuotopic mapping (well-organized mapping of visual space onto neurons) [11, 22]. In addition, the receptive field on the cortex can be covered by more electrodes due to the magnification factor of the primary visual cortex (V1), meaning that larger cortical tissue is given to a provided visual angle [11]. Thus a microelectrode array in V1 can sample a small region of visual space. Extrastriate visual areas (discrete cortical areas located in primary visual cortex) contain retinotopic maps that are smaller in terms of cortical tissue size while they have a larger receptive field than those in the primary visual cortex (V1) [11, 23–25]. This gives the opportunity to sample a large region of visual space by implanting a multi-electrode array such as *Utah arrays*, as illustrated in figure 1.2. Visual area V4 is the best candidate for this purpose because it offers an opportunity to recover the location visual stimuli and it responds well to stimuli of low to medium complexity [26–29].
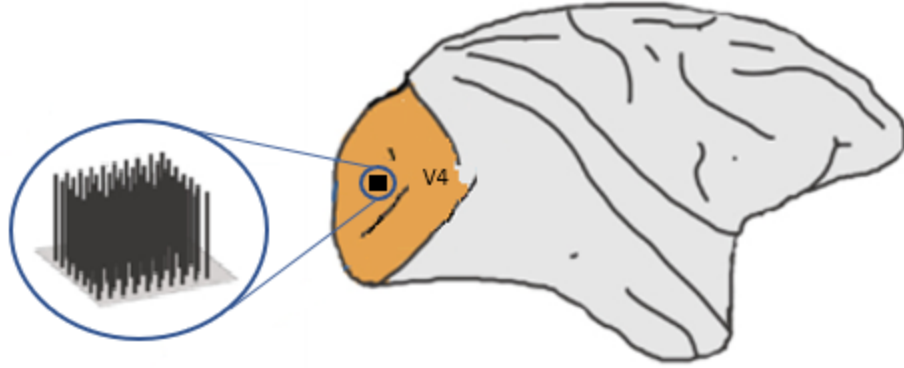
Figure 1.2 **Graphical scheme of implanted electrode arrays.** In the visual cortex area V4 to electrically stimulate the brain, phosphenes induction, and vision restoration.

1.3   Spatial localization

One of the main goals of cortical visual prostheses is to provoke a meaningful percept from phosphenes by applying electrical stimulation to the visual cortex. Studies on phosphene induction in blind patients show that the perceptual properties associated with phosphenes are shape, size, brightness, colour, flicker, spatial location, multiplicity and edge [2]. The generation and detection of phosphenes are one of the existing challenges in using spatiotemporal electrical simulation [2], and to compromise such challenges understanding all aspects of the visual prosthesis is needed.

Phosphenes move with eye movements [2, 5, 16, 18–21]. In a case where six phosphenes were generated simultaneously, all were shown to move with each eye movement [2], which makes phosphenes mapping complicated. Thus, it is necessary for eye-tracking technologies to make sure about image stability during eye movements.

Each eye movement creates a shift in the retina's visual image. There is evidence that all parietal neurons respond when an eye movement contains the site of a previously generated stimulus into the receptive field [10]. However, we are unaware of this shift, thanks to our brain constantly operating adjustments of this displacement, which yields a stable percept of the world [10, 15]. However, many studies report the mislocalization of a visual stimulus that occurs just before a saccade [10]. To find a neural mislocalization, we need to understand neural localization and consequently to show this phenomenon on the visual prosthesis, as it

follows to provide a basic sense of sight, similar to the real visual system. Using electrical stimulation to create significant perception needs two major steps:

(1) To select electrode subsets, in order to provide an electrical current with the required pattern for phosphene generation (localization);
(2) to set the amount of change in intensity and amplitude for each of the electrodes in a subset over time.

To address the delivery of a continuous perception in visual prosthesis applications, an effective microstimulation strategy is needed. This study examine the localization (first step) during saccadic eye movements and the effect of peri-saccadic mislocalization phenomena on decoding in order to provide the required strategy to apply for artificial visions.

In this work, we focus on Multiunit Activity (MUA) and Local Field Potentials (LFPs) responses from extrastriate visual area V4, as it has large receptive field sizes and receives combined responses (MUA or LFP) from various sites, and the capability for fine and coarse discriminations of positions [11]. In addition, early studies have reported that neural activity in LFPs is equivalent to the dissemination of microstimulation effects in the cortex on a 400 micron scale [11, 30].

As it has been mentioned before, perceptual space is distorted by saccadic eye movements. The perception of the position of the visual object presented around the time of eye movements is changed. Perisaccadic mislocalization, is an essential mechanism to reproduce the perceptual stability of a human visual system [3, 10]. To have visual systems similar to the natural one we also need to account for such a phenomenon in visual prosthesis applications.

The contribution of each electrode in the array for a given phosphene has been established by assessing the so-called Weight Fields (WFs). In the first step, we studied the mislocalization problem in weight fields, which illustrate each electrode importance to a given phosphene activation, in order to extract the electrode subset necessary to generate the same stimuli. In the second step, we studied how well these weight fields behave in response to the visual receptive field despite the existence of a transient shift in receptive field (RF). This study can be helpful in the development of visual prostheses,, with respect to its intention to work as a human visual system, by showing the similarity of percept induced by electrical

stimulation and evoked by visual stimuli corresponding to the neuron's receptive field at the microstimulated site [30–32].

1.4 Remapping

The receptive field (RF) of a neuron is defined as the limited region of the visual field whose illumination makes the neuron to fire. A receptive field (RF) describes a particular region determined by degrees of visual angle on the retina and in the visual field. For the first time, Hartline [33] studied the neural mechanism of vision and specifically the representation of space in the visual system based on the retinal ganglion cells of a frog's eye.

We are exploring the world over a series of saccadic eye movements. These movements make changes to the object's locations in retinal space and consequently changes in the position of visual receptive fields around the time of a saccade [3, 10, 15, 34, 35]. The representation of visual space is stable during fixation. However, on presaccadic to postsaccadic eye movements, the cortical representation shifts into the next fixation. The displacement on the retina which corresponds to the saccade occurrence is characterized by the size and direction of the eye movement. Goldberg *et al.* 1992 [10] introduced remapping of the receptive field (RF), according to each eye movement which indicates that neurons can respond to stimuli (probes) flashing in their future receptive field (the postsaccadic receptive field). This phenomena has been introduced as a potential solution for the retinal displacement [10]. The phenomenon of receptive field remapping received wide attention because it was a way for the visual system to reach perceptual stability [3].

Remapping is a neural mechanism by which neurons update their responses around time of saccade to explain the stimulus shift in the retina during eye movements. At the time of saccade the position of neural receptive fields transiently shift toward the saccade target. The remapping phenomena involves the transient shift in the position of each receptive field, towards the location of saccade target, termed future field remapping [3]. On the other hand, Tolias *et al.* 2001 and Zirnsak *et al.* 2014 [36, 37] showed that receptive field remapping called *saccade target* remapping is directed towards the saccade target without considering the position of future receptive field.

Although Goldberg and colleagues were the first ones reporting remapping in lateral intra-parietal (LIP) cortex, there were various studies implying such a mechanism in a different area of the visual cortex [3, 38, 39]. Neupane *et al.* 2016 [3] stated, in V4, that the visual receptive field remaps around the time of saccades with a transient shift towards the saccade target. Also, they reported the existence of both types of remapping (future field and saccade target remapping) on visual cortex V4. In this thesis, the same behaviour for the weight field around the time of saccade is reported, which may help, in the decoding process, for the selection of electrode subset to produce electrical pulses in terms of phosphenes apparition in the visual prosthesis.

This thesis contains five chapters. Chapter 2 provides a literature review on the topic under study. Chapter 3 goes through the detail of methods applied in this thesis. Chapter 4 presents the results of the coding strategy used by the decoder for localization in fixation and saccade preparation conditions. We will present and compare the effect of perisaccadic mislocalization on decoding weights and compare that to the receptive fields. Finally chapter 5 concludes this study and we will talk about possible future work.

CHAPTER 2   LITERATURE REVIEW

This chapter provides a literature review of the visual system and the visual cortex. Also, the history of recording from animals to assist in generating the artificial vision is reviewed. The chapter ends with introducing the review about mislocalization and remapping phenomena that are two main challenges for this thesis.

2.1   Visual system

The visual system is a sensory system that observes the surrounding environment's images by using radiation light. This light has a specific amplitude, frequency, and wavelength. The human visual system has the ability to convert these electromagnetic waves into relevant images. Light waves, to reach the retina, first enter the eye through the cornea and then go through the pupil. The visual system contains three main parts: the eye, the lateral geniculate nucleus or LGN, and the visual cortex [40–42]. The visual system builds a representation of the surrounding environment by interpreting the optical spectrum which is visible for human [43]. Light is transmitted by the lens and cornea, then it will be focussed on the retina as a small image [40]. The image is converted into electrical pulses by the retina and is carried by the optic nerves which connect the eye to the brain. In other words, the transmission of light rays creates images in the eye. The creation of images in the eye takes place in the retina according to fundamental optical properties.

The retina is composed of multiple layers and light waves spread through these layers. Photoreceptors respond and affect the potential of the membrane of bipolar cells. Ganglion cells trigger action potentials that propagate to the rest of the brain via the optic nerve. The ganglion cells are the primary retinal neurons that evoke action potential. These cells have the capacity to recognize the combination of colours, light and dark areas. For the first time, in 1941, Hartline studied the representation of the visual system on frog's ganglion cells [33]. He defined the receptive field as a restricted part of the visual field which causes a neuron to evoke [3, 33]. Therefore, the receptive field (RF) describes a certain area calculated in terms of degrees of visual angle in the retina and the visual field [3]. A few years after, Hubel and Wiesel in 1977 [44] proposed a mechanism to explain the architecture of receptive field and in 1995, Alonso and Reid [45] found the neurophysiological proof for the proposed architecture.

The existence of two visual systems for localization and identification was proposed by Schneider in 1969 [46]. Then, in 1973 Ingle studied the existence of two separate mechanisms for visual systems in frogs, as well as in monkeys which was confirmed by Trevarthen in 1968 [47]. In 1982, the notions of ventral (what) and dorsal (where) streams were identified as processors of spatial and visual features respectively by Mishkin et al. [48]. Later, in 1992, Milner and Goodale [49] replaced the definition of these streams. They proposed the ventral as a stream that computes a map of the surrounding environment which is usable in cognitive operations, and the dorsal stream as a transformer of visual information [50].

The dorsal pathway (where stream) starts from the primary visual cortex (V1) in the occipital lobe and continues up to the parietal lobe [51]. The ventral pathway (what stream) which is related to object recognition, also starts from the primary visual cortex and forwards into the temporal cortex [51].

2.1.1 Visual cortex

The visual cortex is the primary cortical area of the brain where the visual input from the retinas can be obtained, segmented and processed [52]. It is located in the occipital lobe which is in the posterior area of the brain [53]. The visual cortex is split into 5 areas, V1, V2, V3, V4, and V5 [54]. In the visual cortex, neurons evoke action potential, responding, as soon as visual stimuli appear in their receptive field (RF). Neurons located in distinct visual areas respond to different kinds of stimuli. Neurons located in area V1 respond to edges and lines [55]. The main area of the cortex in visual processing is the primary visual cortex or V1 and the occipital lobe areas surrounding the primary visual cortex i.e., the extrastriate visual cortex which contains V2, V3, and V4 [53]. V1 is composed of 6 layers as a function of cortical depth, each layer associated with a different functionality [54]. Figure 2.2 illustrates the visual pathway that is responsible for converting received light energy from retina into electrical action potential which is interpretable by the brain.

V1 receives retinal visual information from the LGN through layer 4 [54] and sends signals to the extrastriate visual cortex. Anatomically, V1 occupies quite a large part of the visual cortex [30, 56]. The extrastriate visual areas have smaller retinotopic maps in comparison with the primary visual cortex and their receptive fields are larger than V1 [24, 25, 57]. V1 transfers this information (or pulses) into the two pre-mentioned pathways (dorsal and ventral
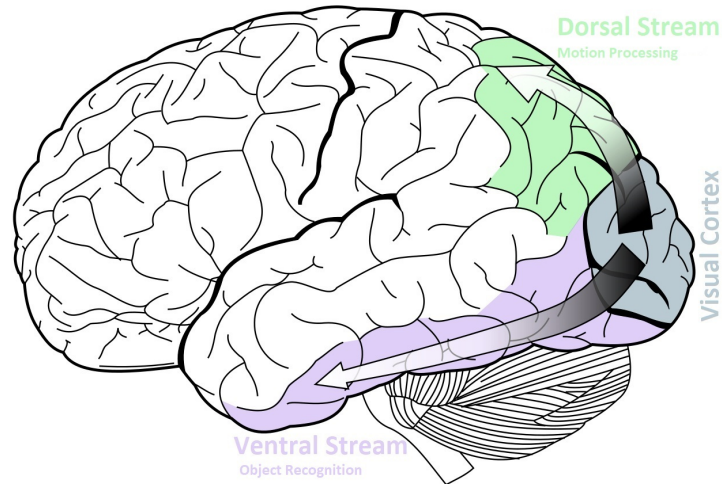
Figure 2.1 **Schematic of visual cortex.** Visual cortex takes a huge amount of cortex and contains two parallel pathways (processing streams). Dorsal and ventral pathways have been shown by green and purple respectively. The visual cortex also has been illustrated by grey. The picture is taken and modified from Wikipedia, made by Selket under licence CC BY-SA 3.0.

streams) [58]. The ventral stream, or what pathway, is started from V1, goes through V2, then V4, and then to the inferior temporal cortex (IT). This stream is related to object recognition [51]. The dorsal stream or where pathway begins with V1 and then it goes through V2 and then to V5 and V6 before reaching to the posterior parietal cortex [58].

Most of the current visual prosthesis applications is addressing the early visual system like V1, LGN, or the retina. The reason for targeting these areas is the fact that given they each have a visuotopic mapping, encoding pixels as phosphenes are simpler [59]. Besides V1, the extrastriate visual cortex also has a role in visual perception [2]. Stimulating in the extrastriate cortex could be a substitute for the prosthesis in the primate visual cortex due to their properties [60]. Some of these properties are, selectivity [61], plasticity [62], specialization [2], and multimodality [63, 64]. Neurons located in the extrastriate cortex show almost the same selectivity as that in V1. For example, a feature that can activate a large number of neurons in V1 can activate a small population of neurons in the extrastriate cortex [65].

This feature can be useful in generating visual percept with the assist of electrodes, in the sense that we would need a lower number of electrodes [61]. In addition, previous studies
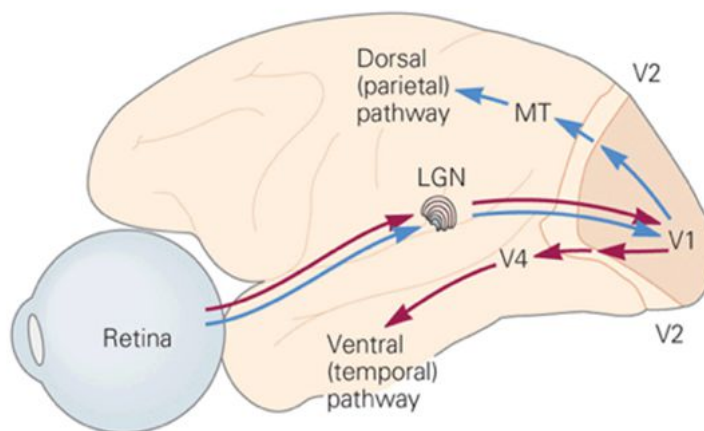
Figure 2.2 **Visual pathway schematic.** In the visual pathway, retina carries out spatial, temporal processing on visual inputs. By receiving information from the retina, it sends visual information to the Lateral Geniculate Nucleus (LGN) through optic nerves and information projects to the visual primary cortex where the visual information is getting processed. Any dysfunctionality in the process of the visual pathway causes visual impermanent. The picture is taken from brain-for-ai.fandom.com, under licence CC-BY-SA.

reported higher plasticity in the extrastriate cortex than area V1 [62]. This can help the brain learn to perceive artificial stimuli reaching higher-level regions [2]. Also, neurons in V1 activate only by visual signals. Thus, for a blind subject, these neurons could be activated through artificial stimulation which complicates the development of an encoder [2]. On the other hand, although neurons in the extrastriate cortex receive inadequate but reliable non-visual inputs, they have comparable stimulus selectivity to that of the visual inputs [63].

As has been mentioned above, the primary visual cortex area is large in comparison with recording arrays. Consequently, a small region of visual space in V1 can be sampled by a multielectrode array. However, the extrastriate visual cortex contains retinotopic maps which although smaller have receptive fields are larger than the ones that are located in the primary visual cortex (V1) [23, 24]. This property helps in sampling a larger region of the visual field. Specifically, V4 which is located in extrastriate contains a retinotopic map of visual space [11]. This cortex can recover the position of static stimuli [26, 30] and respond well to stimuli with low to average complexity [11, 28, 29]. Also, visual cortex V4, is modulated by attention and eye movements, and the attention effects have an essential role in remapping and perisaccadic vision [66, 67].

2.2 Cortical visual prostheses

With an estimated 39 million individuals globally suffering from permanent blindness in 2010 [68], blindness is a widespread cause of extreme visual deprivation. Utilizing direct electrical stimulation of the visual pathway with the assist of artificial devices is one of the possible solutions for vision restoration [2, 68]. Cortical visual prostheses are based on the possibility of performing electrical stimulation in the visual cortex which can map visual percepts called phosphenes [19]. In recent years, stimulating different parts of the brain, with demonstrations mostly done in the primate visual cortex, garnered the interest of scientists [69]. Although electrical stimulation can be applied to various parts of the visual pathway like the retina, LGN, visual cortex, etc. The primary visual cortex (V1) remains an ideal candidate for implanting electrode arrays as it has a large area for implantation of electrodes and in comparison with the other areas is easy to access [2, 70]. Electrical stimulation of visual pathway with multielectrode arrays, also offers the potential of inserting spatio-temporal activity pattern which produces a perception of images that have been made by phosphenes [2, 21, 71].

One of the major problem in cortical visual prostheses development is producing dense electrode arrays covering the visual cortex [19, 56, 72, 73]. Also, a major challenge is to identify stimulation parameters that affect phosphene characteristics, like stimulation frequency, pulse amplitude and etc [2]. The perception of a phosphene image involves the activation of several phosphenes with a particular spatial mapping and brightness. For this purpose, different electrode activation adapted to a predefined pattern is needed [2]. On the other hand, offering artificial percepts very close to natural vision is the other significant difficulty of cortical visual prostheses applications because of the complexity of the visual system [6, 74, 75]. Although, there are many proof of concept clinical trials that show that artificial vision in blind subjects helped them in performance of basic tasks [76–78], still many of these devices fail in updating visual information to provide a perception that is interfacing with the natural visual world specifically during eye movements [4].

To generate artificial visual percepts that interface with the natural vision, the image made by visual prostheses devices needs to change immediately during eye movements or saccade [79]. Otherwise, without considering saccade in artificial visions, the image will be perceived to be unstable by the user [80]. Consequently, prostheses applications need to take into account the updating of the artificial percepts based on the patient's eye movements [81].

2.3 Recording from macaque monkey

Current vision studies attempt to explain the mechanisms of the brain that help us to recognize and remember the world and how vision is altered during injury or degenerative brain diseases [82]. Even though scientists are aware of how information is transmitted by nerve cells in the brain, less is known about how this information is turning to a representation of a particular object [83].

To understand the mechanisms of the human brain, macaque monkeys are used broadly in scientific studies and they have been primate models for studying neural mechanisms in cognition since 2000 due to their similarity to the human brain. [3, 82, 84, 85]. Macaque monkeys are appropriate in studies in studies about vision, the similarity of the visual cortex, the ability for sensory processing, and their ability to respond to visual stimuli [86]. Dacey. 2000 and Troyk *et al.* 2003 showed the striking similarity of macaque monkey's visual cortex functionality [71] to humans which is critical in the visual recognition process [30, 56, 71, 82]. However, this similarity is not limited to the visual cortex. In 1991, Garey et al. reported the similarity of the macaque monkey's lateral geniculate nucleus (LGN) to humans. Later on, Casagrande and Kaas in 1994 and Lubbers et al. 2012 stated that they found a close resemblance in striate cortex V1 between macaque and human. One of the advantages of using macaque monkeys in scientific studies related to the visual cortex is the easy accessibility of visual field representation on V1's surface with electrode arrays [2]. While for cognitive neuroscience studies, other methods like fMRI, DTI can be useful for understanding the human brain [83], they cannot be used in studies that require direct recording from cells [83, 87].

On the other hand, recording directly from cells with electrodes in the human brain is limited due to ethical and functional reasons [87]. For example for the cases to record from electrodes implanted always there are strict limits to electrode implantation associated with the patient's clinical well-being. [87]. While, Feng et al, 2020 showed that using animals limits our knowledge in higher human brain functions like emotion, and social interaction. Using animal can have a strong impact on our understanding of cellular and neural systems [82,83].

2.4 Mislocalization

We move our eyes to scan and capture the information in the world around us [4]. These sudden movements are ballistic and in 1901, Dodge [88] was the first one who named these fast changes of the eyeball position, saccadic movement. Despite the fact that objects positions in the retina change as soon as the eye moves [6], the brain provides us stable and continuous images of the visual scene [10]. In the words of Mach in 1897, *" the whole of space appear as a continuity and not an aggregate field of vision."* [89]. Many scientists studied the mechanism of the visual system which can provide us stable percept with the existence of eye movements. In 1867, Hermann von Hemholtz reported that an incorrect decision was drawn based on a modified visual perception when a patient with disabled eye muscles attempted to move his eyes [90]. Leigh et al. 2015 illustrated that the saccadic eye movement addresses the issue of intense blurring problems, which results in a seamless vision of the visual field [91].

In 1996 Deubel et al showed that the ability of the visual system to identify tiny spatial displacements of a target was found to be strained by saccades [92]. Also, Matin et al. 1965 showed that a visual stimulus presented just before the onset of the saccade, is mislocalized toward the saccade target [93]. Many authors believed that this displacement is a failure of the visual system in remapping the presaccadic to postsaccdic coordinate system [94–96]. On the other hand, numerous authors believe that perisaccadic mislocalization in the visual system is related to the dynamics of the receptive field in the different cortical areas. For instance, in 1992, Goldberg *et al.* reported perisaccadic changes in the receptive field's centre and size in the lateral intraparietal cortex (LIP) [10]. Five years later, Umeno et al. 1997 showed the same changes in the frontal eye field [97]. And in 2001, Tolias et al. stated that in visual cortex V4, before the onset of saccade the receptive field diminish and shift towards the saccade target [36]. The mislocalization phenomena represent transient process errors that create spatial stability through eye movements. It may result from errors in reference signals related to the direction and amplitude of the saccade or the visual reconstruction processes based on the location of the saccade target [98]. In response to the question regarding the neural mechanism which guarantees visual stability without our awareness during saccadic eye movements, Goldberg *et al.* 1992 reported remapping as a visual system solution for the displacement of the retinal image and the blur on the retina which is the result of saccade [3, 10]. Therefore, to generate a stable percept with visual prosthesis applications that would like to be comparable with the natural one, we need to investigate remapping phenomena in our prostheses applications.

2.5 Remapping

With each saccadic eye movement, the position of an object changes in the retina [6]. Although this prediction concept has been studied since 1976 by Wurtz et al. [99], 1980 by Mays et al. [100], and then in 1990 by Goldberg et al [38], in 1992, Goldberg *et al.* for the first time introduced the receptive field remapping as a possible solution for this displacement [10]. Remapping is a neural mechanism in the brain which helps in compensating for the shift in the retina due to eye movements. This remapping is derived from a large neural circuit involving the parietal and frontal cortex [101].

Remapping requires a transient shift from the presaccadic to the postsaccadic spatial position of a neuron's receptive field (RF) [3]. Also, they found that the receptive field's remapping phenomena lead to perceptual stability in the lateral intraparietal cortex (LIP) [10, 102]. It has been demonstrated that neurons in the LIP area respond to a stimulus or a probe that is located at their receptive field (RF) and displayed before the saccade. In other words, the current neural receptive field knew its later position relating to the future saccade vector [10].

The remapping phenomena is interpreted as the brain solution for acquiring visual stability with a combination of visual and eye movement information like: the retinal signal which is due to the position of a stimulus on the visual field and the amplitude and direction of saccade [3, 103]. However, a remapped neuron may transiently respond to a probe anywhere in the visual field as saccade can be performed in any amplitude and direction and this breaks the rules of the topographic organization of the receptive field (RF) [3]. Although many of the previous studies about remapping phenomena were applied to double-step saccade, Goldberg *et al.* in 1992 used one step saccade which flashed a visual stimulus in the future receptive field (RF) before the onset of eye movement [10]. This study helped in understanding neural responses to the future field stimulus [3]. Consequently, Wurtz in 2008 stated that remapping phenomena has an essential role in visual stability and it is a special property of eye movements [9]. Subsequently, this approach was repeated in some other brain areas. Convergence remapping has been considered a special feature, particular to visual cortex V4 [36] as it is famous for being modulated by eye movements and attention [104, 105].

CHAPTER 3   METHODOLOGY

Data used in this master thesis was obtained from a previous study investigating the saccade phenomenon [3]. In this work, the same data was re-analyzed within the context of probe localization for phosphene induction in visual prostheses applications. In this chapter, first, the preprocessing steps are explained. In the next step, the coding strategy is described. And at the end of this chapter, the procedure of analysing the effect of the saccade is clarified.

3.1   Electrophysiological recordings

The recording methods have been elaborated previously in [3, 27, 106]. In summary, a sterile surgery was performed to embed a headpost and a chronic 10×10 Utah Microelectrode Array with 1 mm long electrodes and 400 μm inter-electrode spacing into area V4 of a 8 years old macaque monkey. The arrays were set to cover a significant portion of the parafoveal visual representation. In area V4, the structural and stereotactic coordinates [107] as well as the physiological properties of neurons have been identified [27]. Upon recovery from the surgery, monkeys were rewarded for making visually guided saccades while being chair trained (Crist Instruments). All experiments got approval from the Animal Care Committee of the Montreal Neurological Institute and performed in accordance with the regulations defined by the Canadian Animal Care Council [3].

3.2   Signal acquisition and pre-processing

Wideband signals were recorded on the 96 channels in each Utah series using a standard data acquisition system (Plexon Multichannel Acquisition Processor System), optimised for 10 kHz sampling (hardware filters of bandpass between 0.07 and 2,500 Hz).

An electrode inserted into the brain of an animal detects electrical activity generated by neurons close the electrode tip. The recording ability of each electrode corresponds to the size of their tips. Electrodes with larger tips can record multiple neuron activity. This method of recording, known as "multi-unit recording," is commonly used in conscious animals to monitor variations in behaviour in a discrete brain region during normal activity. The number of cells

surrounding an electrode, as well as which spikes come from which neuron, can be determined using recordings from one or multiple closely spaced electrodes. Spike sorting is the name for this process. This method is effective in areas where specific cell types with well-defined spike patterns exist. Individual neuron activity cannot be distinguished when the electrode tip is much greater, but the electrode can also record a field potential generated by the activity of several cells. Extracellular field potentials are local current sources created as a result of the combined activity of numerous neurons. A field potential is usually generated by the synaptic activation of several neurons at the same time.

Spike sorting and LFP analyzes were performed by digital off-line filtering. The power spectrum of these wideband signals was tracked regularly to reduce line noise and other artefacts [108]. The residual 60 Hz (and potential harmonics) noise was eliminated offline with a previously implemented power spectrum correction system. Preamplifier design adjustment and preliminary signal processing were carried out as previously described [106]. Briefly, spikes were sorted offline by filtering the raw signal between 500 and 4000 Hz on each recording by first bandpass, and then using the modified algorithm 'wave-clus'. [109]. LFP signals were estimated by eliminating wideband signal action potential waveforms using the Bayesian approach [108]; the despiked signal was then bandpass filtered (0.2 to 150 Hz) and downsampled to 500 Hz for generating LFP signals. All the digital filtering was performed with a fourth-order two-pass Butterworth filter. MUA and LFP were extracted offline through MATLAB (Mathworks) and explained in the following sections 3.5.1 and 3.5.2. Figure 3.1 illustrates steps for recording extracellular activities as well as extracting LFP and MUA.

3.3   Experimental paradigm

The experimental procedure has been described previously [3, 106]. A cathode-ray tube (CRT) video projection device with a refresh rate of 75 Hz back-projected the visual stimulus on a semi-transparent display. At the view distance of 78 cm, the projector covered an area of $80° \times 50°$ of the visual angle. All visual stimuli were white square probes with a luminance of 22.5 cd.m^{-2} presented for 25 ms on a dark background with luminance lower than 0.01 cd.m^{-2}. Basic framework of experimental paradigm was illustrated in figure 3.2.

A 0.50° (visual degree) red dot, in diameter, was used as the animal fixation point for each trial in the top right portion of the grid. If the fixation diverged by more than 2.5° from the
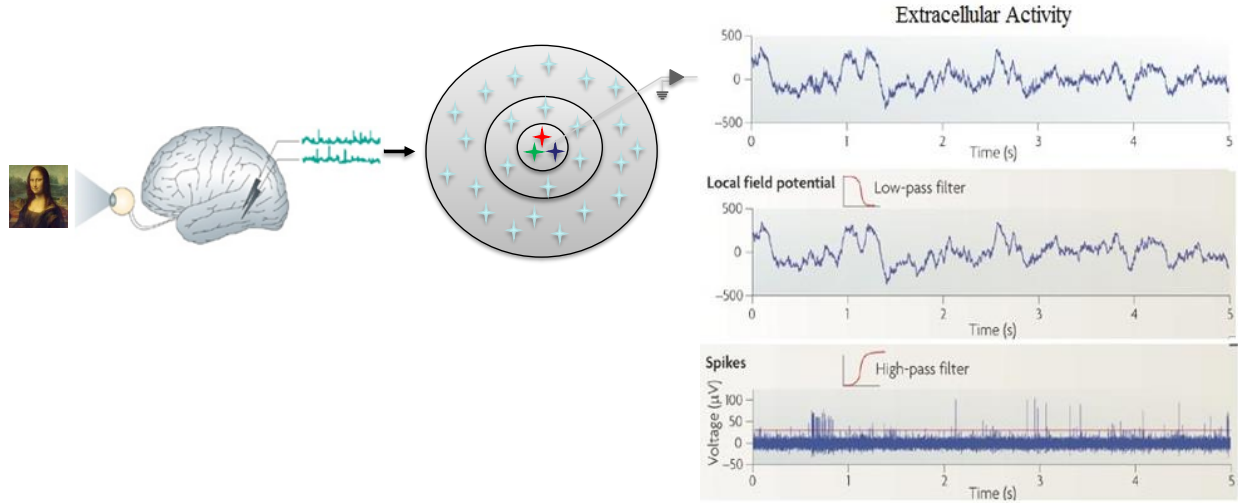
Figure 3.1 **Neural recording.** Neural activities recorded by implanted microelectrode array in the form of extracellular activities after receiving information from the retina by the visual cortex. After the signal is low-pass and high-pass filtered to obtain LFP and MUA respectively for decoding purposes. Picture was adapted and modified from [1].

target, the trial was terminated. After fixing the red dot for 500 ms, a visual sample (probe) was flashed in the lower left quadrant of the visual field, at a location randomly selected, from 100 different positions arranged in a 10×10 grid, as illustrated in section B of figure 3.3. The grid size and position were chosen to mask the retinal eccentricity of the neurons in the lower left hemifield of about 40°. Each probe was square in shape, 2° in width, and located 4° center-to-center distance from its neighbours in both vertical and horizontal directions.

After a variable delay of 500 to 1000 ms, the fixation point jumped to a new target in the top middle of the same 10×10 grid and the monkey needed to make a guided saccade to the new fixation point. Before the beginning of saccade but 100 ms following the emergence of the saccade target's appearance, the second probe was flashed. To ensure the second probe flashes were fully eliminated, a photodiode measured 35 cd.m^{-2} luminance fading on the projection screen. Luminance decreased by 99% 6 ms after the probe offset; any trial in which the saccade began less than 10 ms after the probe offset, was eliminated. During another interval of 500-1000 ms, other stimulus as a third probe flashed for 25 ms while the monkey's eyes were required to be fixated. A liquid reward was given to the monkey after each successful trial ended.
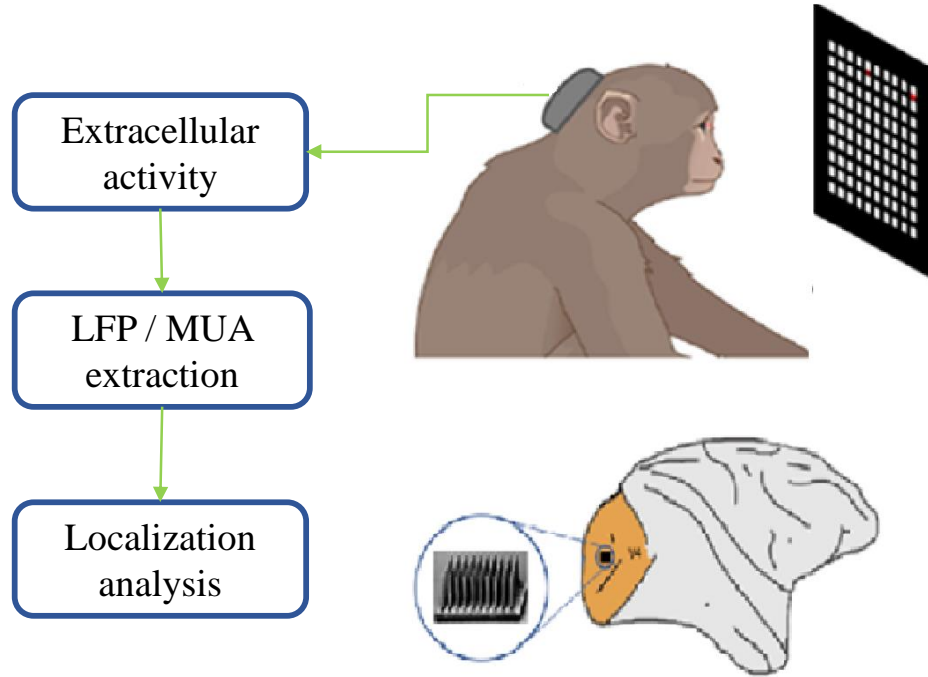
Figure 3.2 **Brief illustration of experimental paradigm.** A basic framework of the experimental paradigm for studying the effect of saccade on probe localization. A monkey with implanted intracortical microelectrode array receives visual stimuli in the time of fixation and saccade in different positions. The resulting activity of neurons, extracellular activity, is recorded. By filtering extracellular activity LFP and MUA responses are calculated. These responses are then decoded for localization purposes. Picture was adopted from [2].

The Liquid reward was only granted if the monkey had successfully made a saccade by further fixation. The test was terminated if the monkey could not fix its eyes within 2.5° from the target. For each fixation point in a pseudo-random order, at least 10-15 trials were repeated per probe location on the grid. To prevent having the same neurons in the various data set, the recording was done on non-consecutive days. Trials containing blinks, double step or catch-up saccade were discarded by offline eye movements processing.

3.4   Eye movements

The location of the eye was tracked at 1,000 Hz by an infrared eye tracker (Eyelink; SR Research). Saccade onset is defined when the eye trace crosses the fixation window and the velocity threshold (200° per second). In contrast, the offset of the saccade was defined by an eye trace velocity reduced below the threshold (200° per second). As mentioned above, the
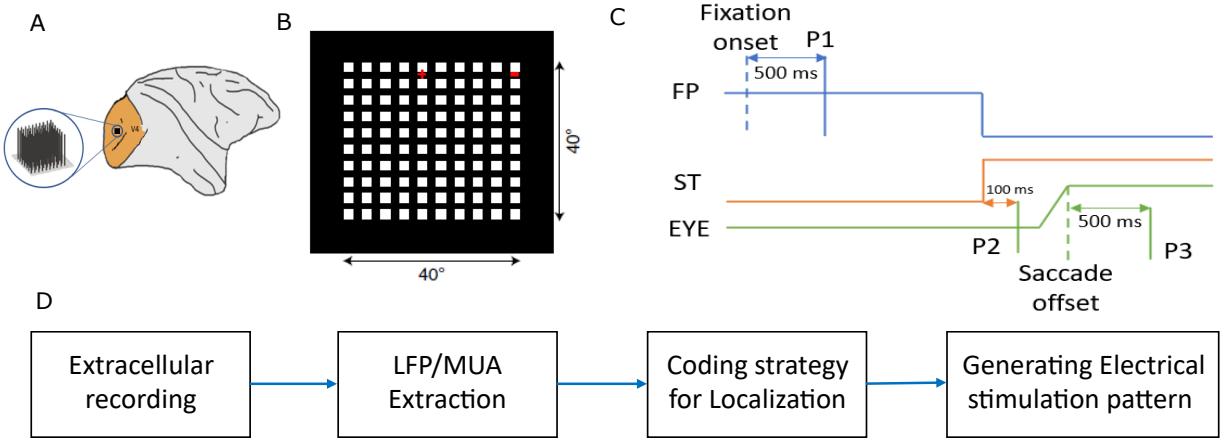
Figure 3.3 **Illustration of experimental paradigm.** (*A*) Graphical scheme of implanted electrode arrays in the visual cortex V4 to electrically stimulate the brain, phosphenes induction, and vision restoration. (*B*) All possible visual probe locations on 10×10 probe grid. Red dot and red + illustrate fixation point and saccade target, respectively. (*C*) Sketch of the time course of a single trial; lines are indicating the relative timing of the fixation point (FP), the saccade target (ST), and the eye movement (Eye). After a random fixation period, the fixation point vanishes and the saccade target emerges and stays on for the rest of the trial. The saccade latency from saccade target appearance was usually 100-200 ms. (*D*) The fundamental process for generating images by phosphenes. (*B*) and (*C*) were adapted from [3].

trial was accepted, as long as the vertical eye trace was in the fixation or saccade window (+- 2.5 degrees). Eye movements have been processed offline to exclude studies that contained blinks or catch-up saccades.

3.5   Data Analysis

All analyses were performed in Python 3.6 and conducted separately for each fixation point. When information observed by the retina and received by the visual cortex V4, implanted electrodes start to record the action potentials from neurons in the form of extracellular activities. By band-pass filtering, these activities LFP and MUA are obtained respectively. See figure 3.1 for the steps of neural recordings.

3.5.1   MUA analysis

Multiunit activity is an extracellular recorded signal. Spikes are the result of action potentials generated directly by neurons. Each electrode records action potential from multiple neurons and MUA or multiunit activity is the unsorted spiking activity that is recorded from the electrode. The recorded neural activity was studied before and after stimulus onset (± 350 ms). Each electrode site displayed the multi-unit activity (MUA) as spike counts computed in non-overlapping time windows of 25 ms. For each trial, the MUA response was presented as the division of the cumulative spike count over a specific time window for each electrode. For MUA, predefined time windows were provided by three different response datasets , wide (150 ms), medium (50 ms) and narrow (25 ms), normalized over all trials per electrode and all began 50 ms after stimulation started.

3.5.2   LFP analysis

Local field potential (LFP) is a transient electrical signal that is generated in the extracellular space in brain tissue by the total synaptic current in an area of the microelectrode [26]. LFP is recorded from the cortical tissue's depths and samples a larger local neuron population. For recording LFP, signals are recorded by implanted extracellular microelectrode at a great distance with an individual neuron in order to ensure no single cell dominates the electrophysiological signal. Then to obtain LFP, the electrophysiological signal is low-pass filtered. Local field potential (LFP) has better localization using its amplitude (0.2 - 150 Hz) than its power in area V4 [26]. Also, the negative amplitude of the broadband LFP signals is effective in distinguishing stimuli in various positions [3]. Hence, LFP responses were specified as the mean amplitude of the broadband LFP signal over time windows similar to that used for MUA. For LFP, three separate response datasets were thus created by predefined time windows that all started 50 ms after the stimulus onset: wide (150 ms), medium (50 ms), and narrow (25ms).

The responses of each dataset were normalized over all trials per electrode. In order to confirm that the location information was not limited to a certain frequency band, a fourth-order Butterworth FIR filter was applied to the broadband LFPs recorded 350 ms before to 350 ms after the onset of the probe [11]. Signals distributed into five frequency bands: theta (4–8 Hz), alpha (8–12 Hz), beta (12–30 Hz), gamma (30–50 Hz) and high gamma (50–80 Hz) separately. The delta frequency band (0.5–4 Hz) was not considered in the analysis as

it could not capture the reactions in each of the three windows. For each band (passed LFP signal) measures and respective datasets were generated. All analyses were performed in Python 3.6 and conducted separately for each fixation point.

3.5.3 Preliminary data analysis

A probe stimulus flashed during fixation (P1), a second probe flashed just before the commencement of saccade (P2), and a third one at the end of saccade (P3). Figure 3.4 illustrates example stimuli (probes) in various positions. After the saccade execution, neural responses to probes (P3) were recorded in different locations on the grid.

We analyzed LFPs and MUA signals recorded from an implanted multielectrode array with 96-channel in visual area V4 of macaque monkeys. For both MUA and LFP traces, the modulation of neural activities was noted in 50 to 125 ms after the onset of the stimulus. LFP modulation appeared in the form of triphasic fluctuations, often with a marked increase in the negative amplitude of the signal, while MUA modulation occurred in the form of increased spike counts. The intensity of modulation depended on the location of the stimulus on the grid (or flashed probe) and varied between recording sites [11].

Each electrode's evoked responses to stimuli (MUA and LFP signals) was calculated from the recorded activities using the narrow, medium, and wide time windows individually. Next, for each probe position, the responses were transformed into z-scores and averaged. Standard score (*z-score*),

$$z\text{-}score = \frac{X - \mu}{\sigma}, \tag{3.1}$$

was calculated in order to standardize responses by eliminating the mean and scaling to unit variance, where, in equation 3.1, X is a training sample, μ is the mean of the training samples, and σ is the standard deviation of the training samples. Standardization is a common requirement for machine learning methods as it helps an estimator to learn from other features correctly.
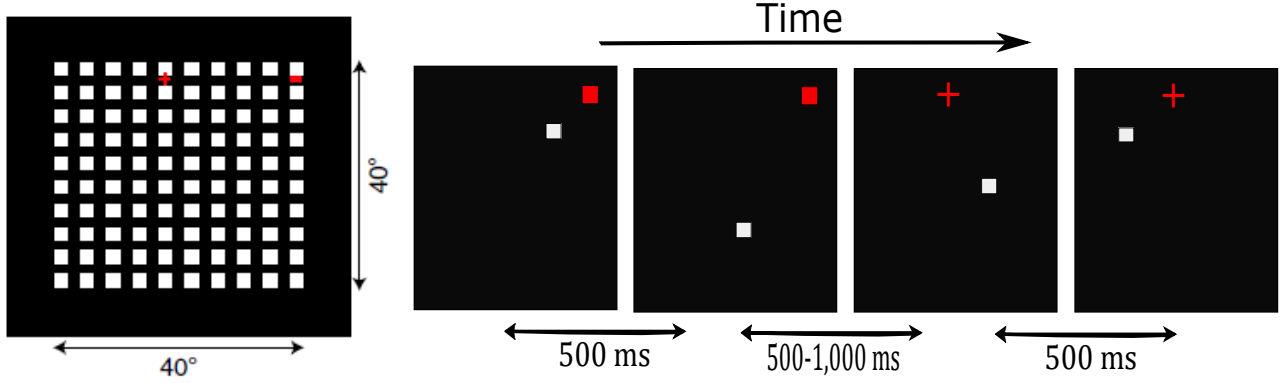
Figure 3.4 **Illustration of probe grid and stimuli.** The left panel shows all possible position for probe appearance on grid with size 10×10 (spanning 40 visual degree). Series of visual stimuli on an example trial; each presented instant displays a probe at an arbitrary position. Red dot and red + indicate the positions of fixation point at P1 and P3 respectively. Image was adapted from [3].

It was shown in [11] that increasing the eccentricity between probes expands the size of receptive fields. However, this effect applies only among the medium and wide time windows. This indicates that the narrow time window does not contain neural response information in visual area V4. In addition, Foroushani *et al.* 2020 [11], demonstrated that response windows of minimum 50 ms are required for obtaining the information about neural responses. Therefore, they showed that, for MUA, the wide window obtained better discriminating performance and that, for LFP, the medium size window is more effective. Besides that, we calculated the localization performance (measured by F_1 score, as explained in the following section 3.7), with all three time windows. As we reported in section 4.1 of the results, for MUA responses, the wide window is more localized, and, for LFP, the medium window has better localization performance for real-time visual prostheses applications. Also, by comparing the calculated performance pattern, given in figure 4.1, with ideal ones, given in section C of figure 3.7, for both MUA and LFP, the wide and medium time windows are the most similar to the ideal performance patterns. Consequently, we analysed the responses using wide windows for MUA and medium windows for LFP.

3.6 Receptive field

As it is described in section 2.5, remapping introduced as one of the natural visual system's compensation solutions for the retinal displacement. During remapping, neurons respond

to their stimuli in their future receptive fields. The receptive field of a neuron defines as a limited region of the visual field whose illumination makes a neuron fire. In order to be able to compare the behaviour of our proposed decoder (explained in the following section 3.7) we computed neural receptive field with respect to saccadic eye movement steps.

To calculate the spatial receptive field (RF) map for each electrode, we averaged the standardized responses over trials with the identical probe position. The calculated receptive field (RF) was then smoothed by a Gaussian filter and linearly interpolated in two dimensions (over the stimuli (probe), 10×10 grid). The Gaussian filter is defined as

$$G(X,Y) = \frac{1}{2\pi\sigma^2} e^{-\left(\frac{X^2+Y^2}{2\sigma^2}\right)}, \tag{3.2}$$

where $\sigma = 0.8$ is the standard deviation, and (X,Y) is the position of each probe on the grid. We then fitted a two-dimensional Gaussian filter on the responses

$$G(X,Y) \sim G(A, \mu_x, \mu_y, \sigma_x, \sigma_y, d) = A e^{-\left(\frac{X-\mu_x^2}{2\sigma_x^2} + \frac{Y-\mu_y^2}{2\sigma_y^2}\right)} + d, \tag{3.3}$$

where A is the maximum response, (μ_x, μ_y) are the coordinates of the central position, SD (σ_x, σ_y) are the standard deviations, and d is the bias. The input and the output of the model are the (X, Y) positions of each probe on the grid, based on the fovea position, and the mean response to each probe, respectively. The centre of each receptive field was computed as the centre of ellipses of full width at half height of the fitted Gaussian with diameters D_x and D_y representing the receptive field [11] such as:

$$
\begin{aligned}
D_x &= 2\sigma_x \sqrt{-2\ln\left(\frac{1}{2} - \frac{d}{2A}\right)}, \\
D_y &= 2\sigma_y \sqrt{-2\ln\left(\frac{1}{2} - \frac{d}{2A}\right)}.
\end{aligned}
\tag{3.4}
$$

The average of D_x and D_y is reporting the diameter of each receptive field.

3.7 Localization analysis

Localizing spatial positions was performed by classifying the responses to the presentation of a specific probe position against the rest of the probes. For this purpose, we used a linear support vector machine (SVM).We used SVM because it is efficient for small datasets as it focuses on support vectors. Despite some linear algorithms like linear discriminant analysis (LDA), the support vector machine has hyperparameters (regularization parameter C) that control the size of margin between support vectors. In addition, compared to other classification algorithms like logistic regression (LR), it is less sensitive to outliers. We applied localization analysis on MUA and LFP separately. SVMs are among the most useful algorithms in large-dimensional cases and in situations where the number of dimensions exceeds the number of measurements.

The dataset was made of 1769 trials (data points or samples). SVMs find a hyperplane that distinctly classifies data points by maximizing the distance between each of them and the hyperplane. We chose linear kernel for our estimator (SVM) in order to localization of each probe position. SVMs define a space with the number of features as the number of dimensions, so we would have 96 dimensional space (96 electrodes). In such a space most probably data are linearly separable. Linear SVM solves

$$
\begin{aligned}
\min_{\omega,b,\xi} & \ \tfrac{1}{2}||\omega||^T\omega + \tfrac{C}{2}\sum_{i=1}^{n}\xi_i^2, \\
\text{s.t.} & \quad y_i(\omega^T x_i + b) \geq 1, \ \ i = 1,...,n,
\end{aligned}
\tag{3.5}
$$

where C is a hyperparameter which trades off between misclassification and margin, equivalent to the complexity of the decision function, parameter b is the bias of the algorithm. Given training dataset are $x_i \in \mathbb{R}^p$, $i = 1...n$, and targets are $y_i \in 0, 1$. The above optimization paradigm finds the optimal hyperplane which maximizes margin between classes.

Our problem is a binary classification schema since we discriminate each probe position versus the rest of the probes located on the grid. The label of the target position is 1 (positive), and the other positions are labelled 0 (negative). By solving the optimization problem given in equation 3.5, 96 weight values ω will be calculated for each electrode. SVM updates the weight values in each iteration of training to minimize the loss function and at the end of the training process will report a weight with the minimum loss as a learned weight per electrode.

Positive weights promote samples to be classified as the positive class (target position) and negative weights lead trials to be classified as the negative class.

To construct a weight field (WF) for each electrode, we positioned the corresponding probe localization weight at the position of each probe. Therefore, for each electrode, we will have a 10×10 grid which has been filled by the localization weight values for each position on that grid, as illustrated in figure 3.5.

The squared value of each weight determines the strength of its (electrode) contribution in the classification (localization of a probe position). We first normalized weights for each probe discrimination (localization). By averaging squared weights of each electrode across all discriminations, i.e. 100 discriminations, we can estimate the overall importance of each electrode. This process helped us to select some of the most important electrodes in order to visualize the original weight values on the grid field (weight field, WF). In cortical prostheses applications when our goal is to localize a phosphene at a particular position, we can use these weights and apply them during microstimulation.

We shuffled the order of the trials in the training dataset to make sure that a random sample is representative of the dataset. Since the number of repetitions of each probe position differed (imbalanced label), we adjusted the SVM weights to preserve the balance of the learned weights in inverse proportion to the class frequencies of the trials by using different hyperparameter C (presented in 3.5) for each label.

We split trials into 80% training set and 20% test set. 5-fold cross-validation technique and Grid-Search were used together to find the best set of hyperparameter (C for each discrimination) in order to prevent overfitting. In 5-fold cross-validation, 4 folds were used for training and 1 held out fold was used for validation. This process was repeated 5 times with each fold assigned once to the validation fold. The average of these 5 performance values was used as the performance using a specific set of hyperparameters (here, C). The model that generated the highest performance was selected for the subsequent analysis. For measuring both validation and test performance, we used F_1 score. Localization process diagram was illustrated in figure 3.6.
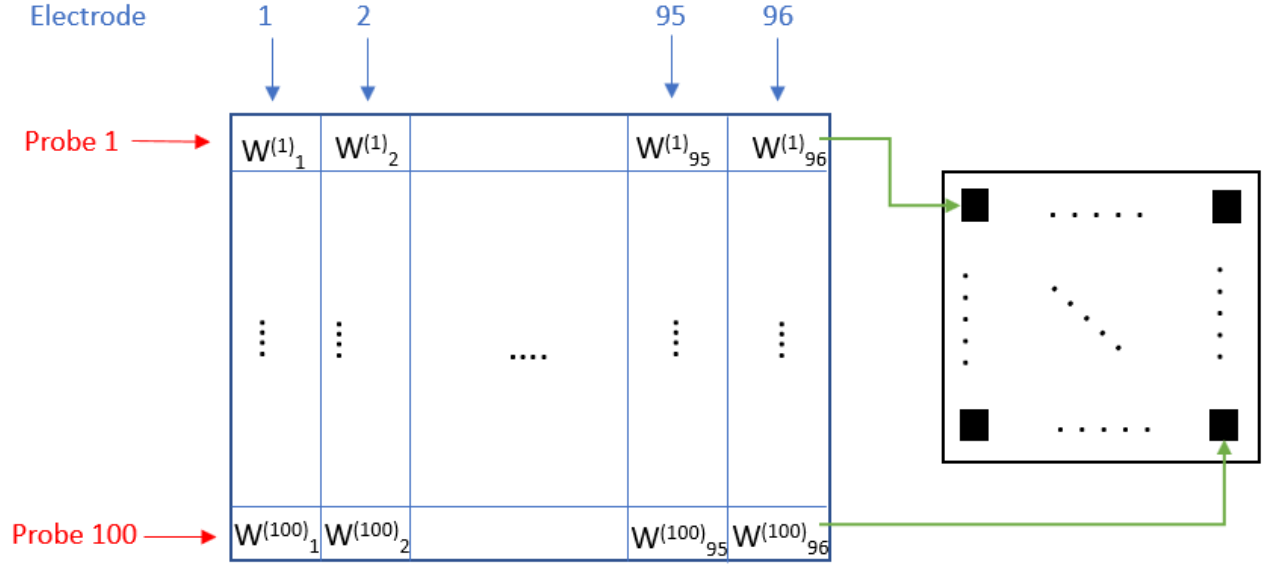
Figure 3.5 **Visualization of weight field.** In the left array, each row is 96 weight values assigned to the electrodes for localizing one probe position. The right square illustrates an example of the weight field (WF) constructed from the left array for electrode number 96. On the right grid, black squares are the representation of each probe position. For each column in the left array, there is a corresponding right square which is the representation of the weight field for each electrode.

F_1 score is useful when we want to classify positive minority classes, from an imbalanced dataset, that are the labels corresponding to the target position. F_1 score is calculated from precision and recall

$$F_1 = 2 \cdot \frac{\text{precision} \cdot \text{recall}}{\text{precision} + \text{recall}} \tag{3.6}$$

where precision shows what proportion of selected items is actually correct and recall answers to the question of what proportion of correct positive prediction is selected. In other words, precision illustrates how many selected items are relevant and recall, shows how many relevant items are selected in the binary classification problem. Mathematical equations of precision and recall are shown in 3.7 and 3.8 respectively.

$$\text{precision} = \frac{\text{true positive}}{\text{true positive} + \text{false negative}}, \tag{3.7}$$
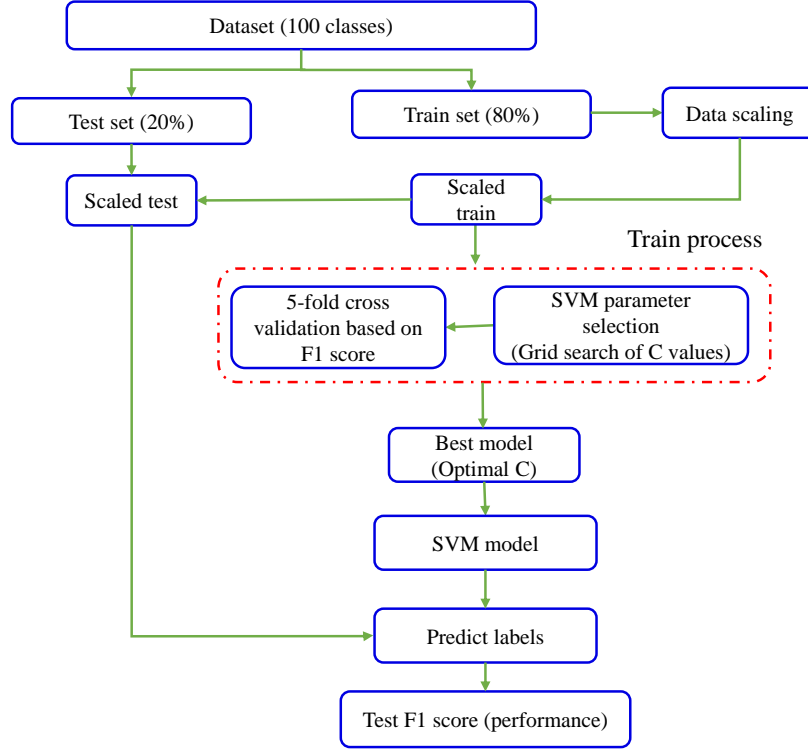
Figure 3.6 **Localization model block diagram.** Dataset was split into train and test sets. The training set was transformed into z-score and its means and standard deviations were used to standardize the test set. In the gridsearch training process, a set of values for hyperparameter C were tried out for use in the cross-validation. fold-averaged cross-validation F1 scores with each C were stored and at the end of the training, C value with the highest F1 score was selected. This optimal model was used to predicted labels. Following the prediction process, model performance was calculated as the F1 score of the model on the test set.

and

$$\text{recall} = \frac{\text{true positive}}{\text{true positive} + \text{false positive}}, \tag{3.8}$$

Where true positive refers to the positive samples predicted correctly (as positive), false negative relates to the positive samples predicted incorrectly (as negative), and false-positive shows the negative samples predicted as positive. F_1 score is using positives and negatives to measure the accuracy of the classification model in its prediction.
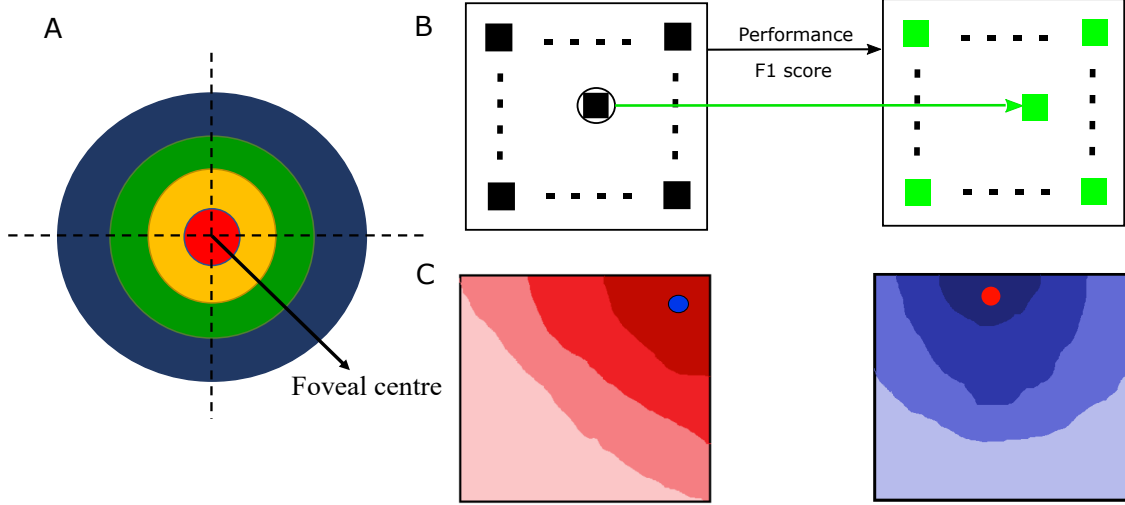
Figure 3.7 **Visualization of localization performance map.** (A) Position close to the fovea centre have lower eccentricity and can be localized better. (B) Discrimination performance for localizing each probe position was presented at the location of each probe on the grid. Black squares are representing probes and green ones are performance at position of each probe. (C) The ideal performance pattern with respect to the retinal position (i.e. blue and red circles). Left and right plots are corresponding to the expected performance pattern in states P1 and P3.

The weighted linear combination of receptive fields (RFs) decides where the probe is localized. $\omega_1 x_1 + \omega_2 x_2 + ... + \omega_i x_i$ (in equation 3.5), where x_i are the response from each electrode i, can be rewritten as $\omega_1 RF_1 + \omega_2 RF_2 + ... + \omega_i RF_i$. This equation suggests that the contribution of each electrode varies for localization of each probe. Mathematically, it is presented as the weights assigned to each receptive field for localization of a position. Weight field demonstrates how well an electrode can localize every position in the visual field. Therefore, an electrode with the maximum receptive and weight fields can best localize a position. Calculated discrimination performance for localizing each probe position was mapped at the position of each probe position on the grid, see section B in figure 3.7. We expected to see extracted performance pattern in P1 and P3 close to the ideal patterns, shown in section C of figure 3.7. In this work, we investigated on the performance pattern for P2.

3.8   Mislocalization analysis

Numerous studies have reported that a position of visual stimulus is mislocalized when it is flashed during the execution of saccade, which causes a change in the receptive field [3,44,110,

111]. Remapping phenomena or spatial updating has been introduced as a brain mechanism for compensating this displacement which has been caused by saccadic eye movements [3, 10, 101]. In order to provide continuous images to offer better perception in visual prostheses applications, we need to investigate the remapping phenomenon on extracted electrodes weights from the proposed model during localization. The representation of the visual scene is stable during fixation. A position on the visual scene can be decoded by a neuron. At the onset of saccade, the representation of the position shifts towards the position of the next fixation. After saccade, the neuron continues to respond to the stimulus. This step entails a remapping of the stimulus from the initial fixation coordinates to those of the desired fixation. [3, 10]. This process is one of the visual system mechanisms to provide a stable visual word.

To investigate the occurrence of mislocalization we need to know if there is any transient shift on electrode's weights (EW) at the onset of saccade as it occurs on the receptive field. For understanding the occurrence of mislocalization we need to know what is the dynamics of the remapping vector during saccade (perisaccadic). Remapping refers to a visual neuron phenomenon that predictively responds to stimuli at the imminence of the eye movement.

Saccade can happen in any direction with any amplitude, so the neural receptive field (RF) can remap anywhere in the visual field. Consequently, corresponding weight fields (WF) can also remap anywhere in the visual field. Studying the future field and saccade target remapping on weight fields will assist in understanding mechanisms of mislocalization in perisaccadic eye movements. To illustrate the transient shift on the weight field, we studied changes between actual and remapping vectors.

The true weight field shift is a vector connecting the centre of the current field (CF) and the centre of the future field (FF). The actual remapping vector connects the centres of the perisaccadic weight field and the future field. To show changes in these vectors we studied the magnitude and angle between them in pre, peri, and post saccade steps, as illustrated in figure 3.8. To calculate the centre of the weight fields we fitted a two-dimensional Gaussian filter to the weight field data. The definition of the Gaussian filter has been described in 3.4.

The angles between the vector $\bar{a}$ of future field (CF - FF) and the vector $\bar{b}$ of actual remapping (Perisaccadic weight field - FF) is calculated as
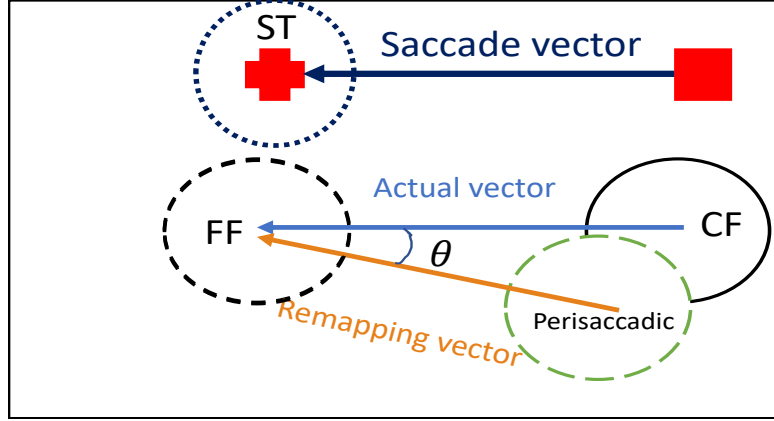
Figure 3.8 **Schematic of Weight field remapping.** A cartoon of the current field (CF)(solid black circle), future field (FF)(dashed black circle), and an example of perisaacdic field (dashed green circle) of an assumptive neuron for an away saccade (dark blue arrow). The actual weight field vector is between CF and FF (blue arrow). Likewise, the actual remapping vector is connecting the centre of perisaccadic field and future field (FF) (orange arrow). θ, represents the angle between the actual and remapping vector. Red square and cross illustrate the first and the second fixation points (saccade target ST), respectively.

$$\alpha = \arccos \frac{\bar{a}.\bar{b}}{|\bar{a}| \, . \, |\bar{b}|}. \tag{3.9}$$

CHAPTER 4   RESULTS

This chapter contains the results of the coding strategy used by the decoder for localization in fixation and saccade preparation conditions. We will present and compare the effect of perisaccadic mislocalization on decoding weights and compare that to the receptive fields. We studied neural activity data recorded from 96 electrodes in 1769 trials. In each trial the data was provided 350 ms before to 350 ms after the stimulus onset. MUA data were spike rate values over 25 ms slots while LFPs data were sampled at 500 Hz rate.

4.1   Position decoding

In this section, we characterized the precision of our decoding strategy to discriminate positions from MUA and LFP responses in V4. We showed our proposed method performance for position decoding which helps to select a minimum number of electrodes required to produce a stable percept during saccadic eye movements for visual prostheses applications. To decode probes positions on the grid, we trained a support vector machine (SVM) on both MUA and LFP responses during fixation (P1), at the initiation of a saccade (P2), and after the saccade (P3). Foroushani *et al.*2020 [11] showed that MUA and LFP responses are capable to decode the position of each probe. We applied the linear support vector machine (SVM) classifier to discriminate neural responses to a specific probe position among responses to the other probes. Our proposed decoder (SVM) assigns a weight to each electrode which shows its importance level to discriminate each probe position, ω (weight) was calculated by equation 3.5.

To select a correct response window for MUA and LFP we compared the performance results for three specific windows (narrow, medium, and wide). In section C of figure 3.7, the ideal pattern for localization performance map (measured by F_1 score) has been shown. Based on this, with lower eccentricity we have higher performance. Our result in figure 4.1 shows that, the narrow and medium windows for MUA responses, comparing to wide window, they have lower localization ability. However, the wide window has a closer pattern to the ideal localization performance pattern. In narrow window of LFP, the performance has not been localized correctly. For LFP, the medium and wide windows both have a close pattern to the ideal one. In addition, in closer area to fovea centre, MUA with the wide time window

is better localized and LFP with medium and wide time windows have better localization performance. However, for real time applications in visual prostheses a smaller time window is better than a wider one [11]. Consequently, we chose a medium time window for our localization purposes.
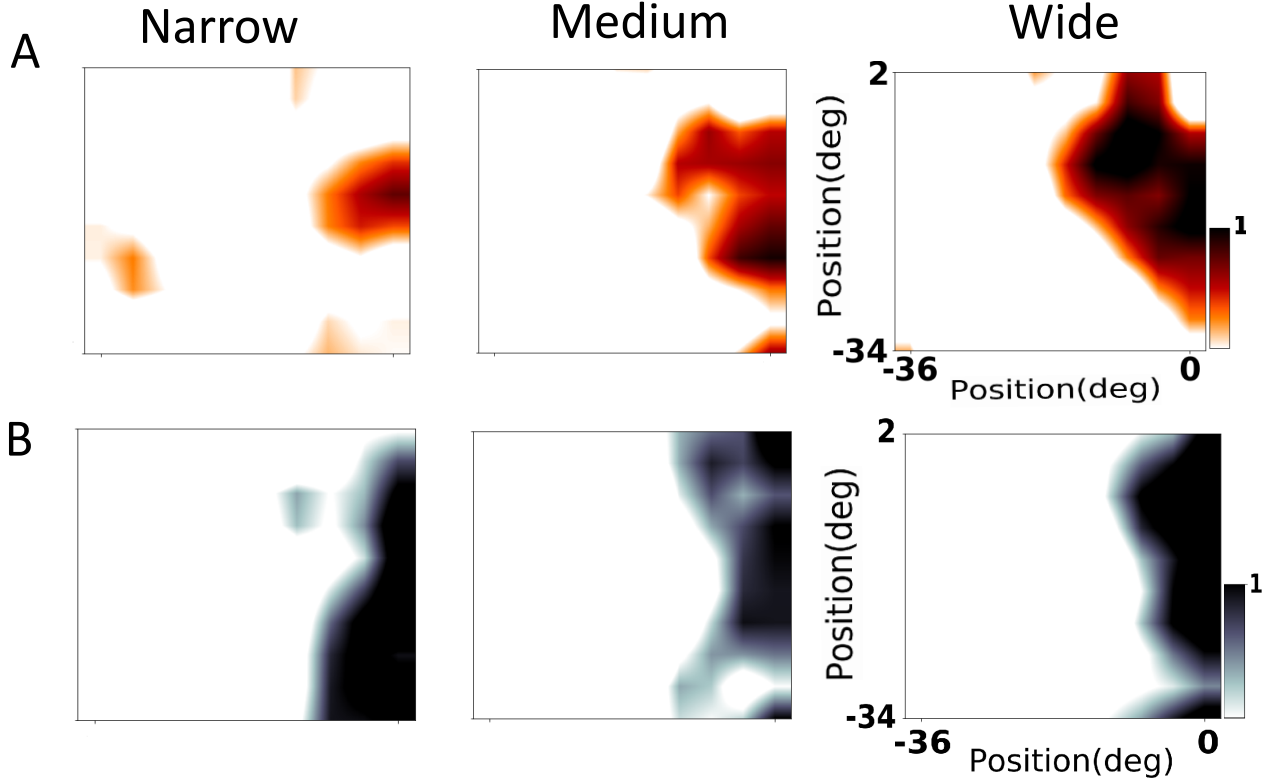
Figure 4.1 **Visualization of performance pattern.** Plots are representing the extracted performance pattern in P1 for three time windows: narrow, medium, and wide. Section A and B corresponds to the performance patterns for MUA and from LFP responses, respectively.

Eccentricity is the distance between the foveal centre in visual degrees. Localization performance depends on eccentricity, in our experimental setup, it is the distance between a position on the grid and the position where the monkey has fixated its gaze. Performance in lower eccentricity is higher, see section (A) figure 3.7; change in the retinal position alters the performance map accordingly. The results illustrate that, by shifting retinal position from P1 to P3, performance maps shift accordingly to keep the highest performance near the new (or target) fixation point (P3). However, this behaviour breaks slightly for P2, as shown in figure 4.2. To calculate the decoding performance we used the F_1 score reported as a number in a range from 0 to 1, as defined in equation 3.6. Figure 4.2 shows the result of the measured performance for the support vector machine (SVM) on both MUA and LFP responses in all

three state of the experiment, P1 (before the saccade), P2 (at the initiation of the saccade), and P3 (after saccade). Our results show the dependency of the position discrimination on the representation of fixation point on pre and postsaccadic eye movement. On the other hand, we can interpret from the measurement how well the algorithm could discriminate each probe position. Table 4.1 reports the localization performance corresponding to lower and higher eccentricity. These values are measured by F_1 score, figure 4.2. In the table 4.1, we reported minimum and maximum performance values to show the effect of eccentricity on the localization performance. Each row of the table reports minimum and maximum values of localization performance and the corresponding probe eccentricity.

Figure 4.3 shows results of the subtracted performance values of P2 from P1. Subtracting performance results of P1 from P2 (P2 – P1) showed a significant drop in the localization performance of probe positions close to the foveal centre in the P2 condition compared to that of P1. This suggests that in the time of saccade, V4 neural activity cannot accurately localize spatial positions. This drop was more obvious near the fovea because farther probes in both conditions (P1 and P2) could not be localized accurately, which makes sense: lower eccentricities have smaller receptive fields (RFs) which can localize spatial positions better.

In order to understand the coding strategy used by the decoder to localize positions, in the next sections we study properties of linear weights assigned to the electrodes by the decoder.

4.2 Localization

Here we focused on phosphenes localization with the assist of electrical stimulation in presence of a saccade, to suggest an effective strategy, very similar to the natural vision, for phosphene induction in the generation of a stable percept in visual prostheses applications. The purpose of localization is to discriminate a probe position among the others on the grid. In other words, localization analysis is classifying group responses for each position (probe position) on the grid.

For cortical visual prosthetic applications, localization weights for each position can help to find correct microstimulation strategy to induce phosphenes at particular position. For the localization of each probe position, 96 weights were obtained. For each electrode observed weight from SVM, defined in equation 3.5, was mapped on a grid as shown in figure 3.5). Our
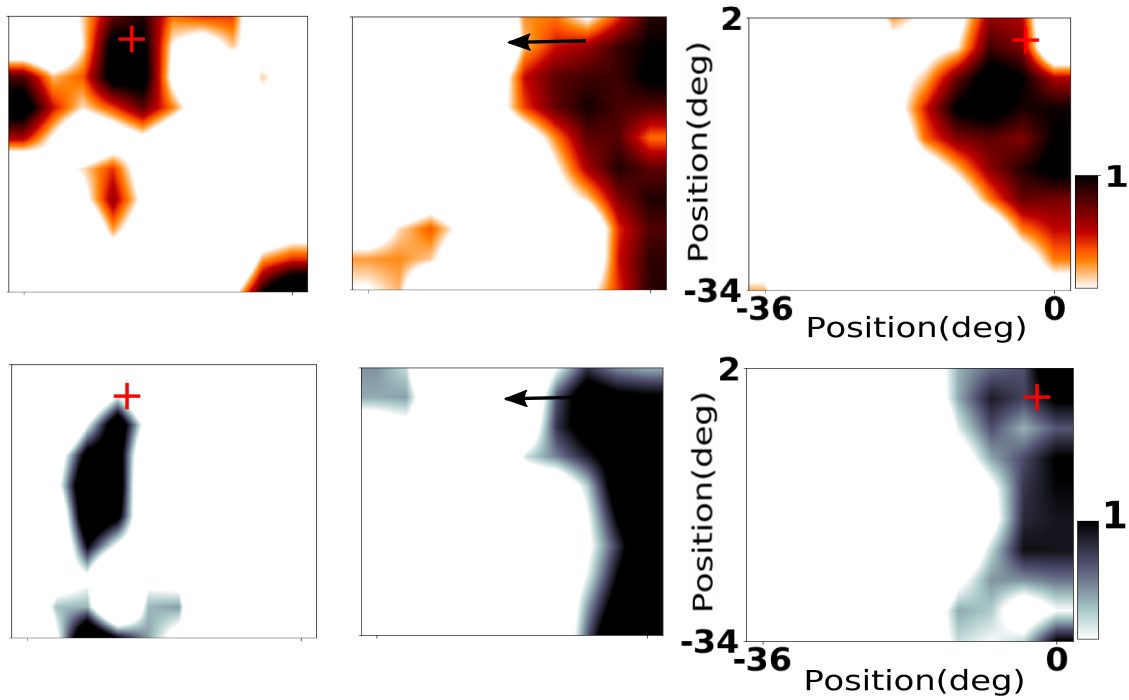
Figure 4.2 **Localization performance in three states.** Fixation on P1 (right), fixation on P3 (left), and saccade onset (P2). Performance depends on the eccentricity so the position of fixation affects the receptive field position. In P2 (onset of saccade), the localization performance has been changed towards the fixation point on the left side of the grid (P3). Performance results for MUA (top) and LFP (bottom) are illustrated.
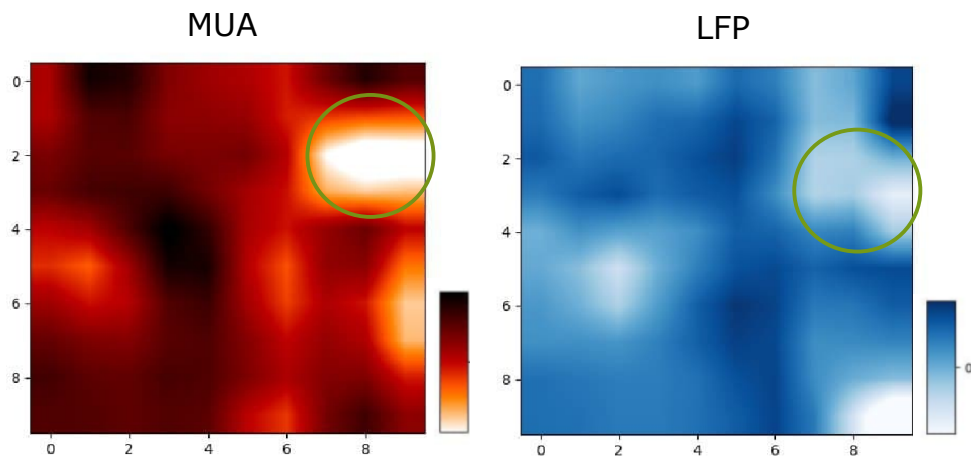
Figure 4.3 **Localization performance drops in the time of saccade.** Above graphs illustrate subtracting performance result for MUA and LFP from P1 by P2. Negative values, show the information missed in P2. The immediate drop close to the fovea centre (top right of the grid) is clearly appears in both graphs through the squares with the lower values.

Table 4.1 **Localization performance with respect to the eccentricity**

Signal	Performance	P1	P2	P3
MUA	Minimum	0.26 (36.055°)	0.06 (39.446°)	0.61 (36.055°)
	Maximum	0.98 (4.472°)	1.00 (10.770°)	0.97 (13.416°)
LFP	Minimum	0.16 (38.418°)	0.25 (31.304°)	0.12 (39.446°)
	Maximum	0.96 (10.000°)	1.00 (4.472°)	1.00 (30.000°)

results enables us to select the best electrode average response over all probes (positions) on the grid in order to choose the set of electrodes to apply a significant microstimulation strategy for every step of eye movements: P1, P2, and P3. Moreover, this method gives the ability to define the best electrode for localizing a specific probe position by means of sorted weights for each of the electrodes. Before performing classification analysis we standardized (z_{score}) the responses associated with each electrode. Thus, this standardization brings responses from all electrodes to the same scale. Those with the highest weight values are the ones that contributed the most. Therefore, not only the best electrode is not the one with the largest response value but also, the most important electrode is the one with the larger weight.

Figures 4.4 and 4.5 show weight fields for MUA and LFP weight fields, respectively, for fixation points (P1, P3) and the onset of saccade (P2), for the three electrodes with the best average responses for each probe position. We choose three electrodes with better weight field (WF) in terms of visualization purposes. After eye movement the relative position of each probe to the fixation point changes. The positions that were close to the foveal centre are not close anymore after jump from P1 to P3, hence the distribution of localization performance changes. Therefore, for phosphene localization in each step of the saccade, we need to activate the electrodes that have the largest weight to localize a specific position.

For each probe position, 96 weights were presented both for MUA and LFP. The extracted weights help in discriminating each position over the others on the grid. With our method, for each step of eye movements (P1, P2 and P3), the best electrode candidate can be selected to localize each position in cortical visual prostheses application. Each probe position elicit response in multiple electrodes and the electrode with its receptive centre at the position of that probe is not necessarily the best electrode. SVM uses information from multiple electrodes to discriminate a single probe position. These results show that our method can be

used to weight electrodes in visual prostheses applications in order to stimulate phosphenes even during eye movements. The generated responses to a probe position (by applying electrical stimulation) are not unique. However, for each probe position, the decoder sets responses in a particular interval that can indicate the response to a probe with a specific probability value. In visual prosthesis applications, for each probe position, the electrode with largest weight values will be selected for the electrical stimulation. However, to localize a probe position it is possible to have multiple electrodes with the same weight values. Thus for phosphene localization, in visual application prostheses, we need to consider all effective electrodes (largest weight value). Or, we can remove electrodes with redundant information [11], to choose the effective ones for phosphene's localization. By stimulating an electrode with the largest weight value for localization purpose, we expect a phosphene to be induced at that position which is necessary for making patterns in visual prostheses. Therefore, with the existence of electrodes with the same weights, we suppose to have the same phosphene induction. Studying the extracted localization weights from our decoder (SVM) enables us to explore the mislocalization phenomenon in order to compare the behaviour of the decoder with the real visual system.

4.3 Mislocalization

As it is mentioned in section 2.4, there are many reports of failures of visual prosthesis applications in updating visual information during saccadic eye movements [4]. Even though the mislocalization phenomenon exists in healthy natural visual systems, our brain mechanisms prevents us to notify it. In prostheses applications, to have such a system proposing a stable image of the world, even in the time of saccade, we first need to investigate the proposed decoder system to induce phosphenes, in order to check if it behaves similarly to the natural visual system during a saccade. In this case, we can claim that our decoder has the ability to provide a stable percept for the visual prostheses application.

As mentioned before, remapping contains a transient shift in the spatial position of a neuron's receptive field from presaccadic to postsaccadic eye movement. This phenomenon have been introduced in 1992 [10] as the brain ability to provide visual stability. In figures 4.7 and 4.8, changes in neural receptive field have been illustrated for pre, peri and post saccade. In state P2, the onset of the saccade, the receptive field moved towards the saccade target. Sujay *et al.*, 2016 [3] reported that, in the onset of the saccade, the centre of the receptive field will shift. This shift can be noticed in figures 4.7 and 4.8 for MUA and LFP, respectively.
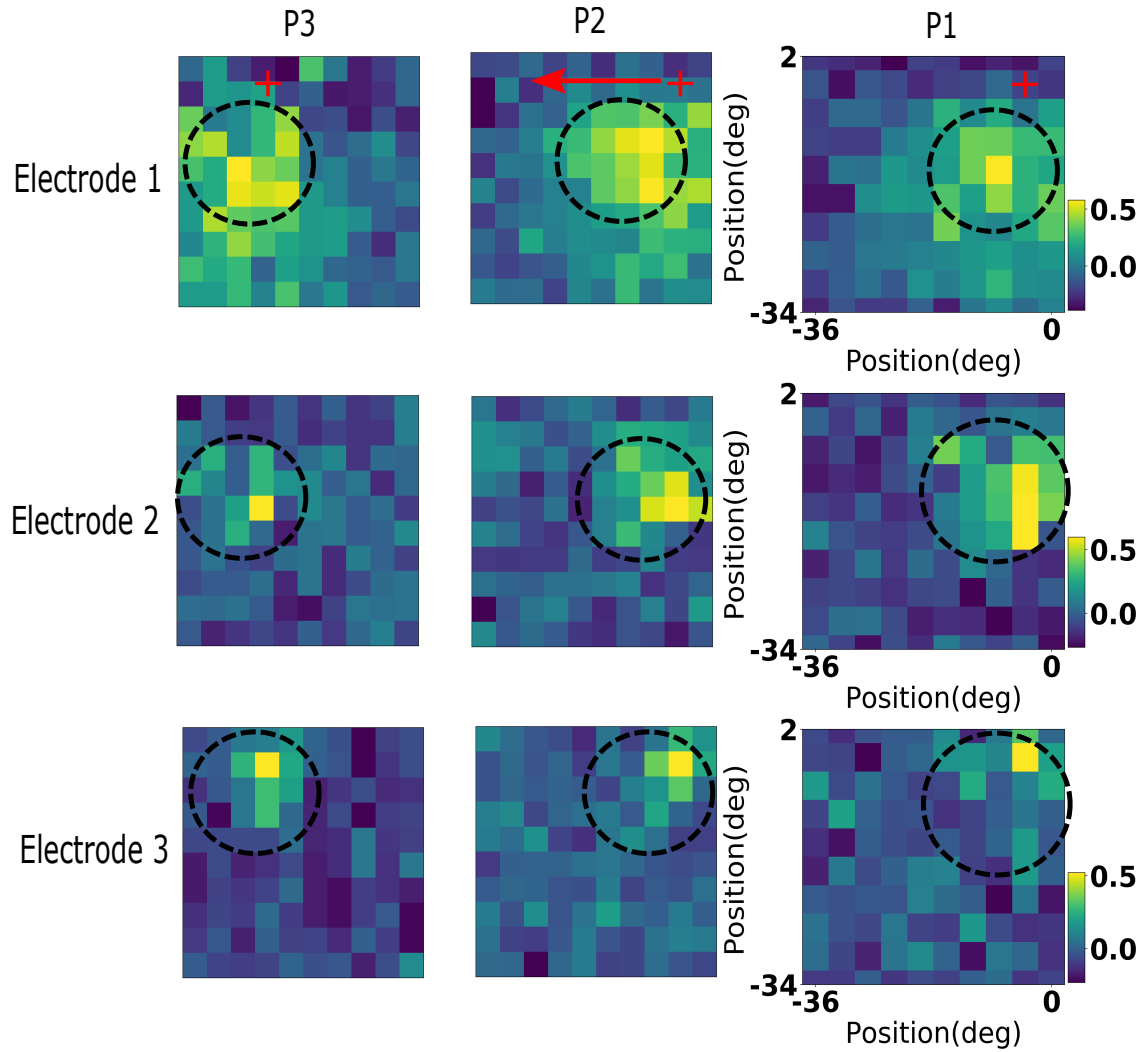
Figure 4.4 **Weight fields with respect to MUA responses.** Calculated weight values for each electrode, for localizing each probe position, have been illustrated in the location of visual stimuli for P1, P2 and P3, using MUA responses. The three selected electrodes, are sampled out of 96 for better visualization purposes.
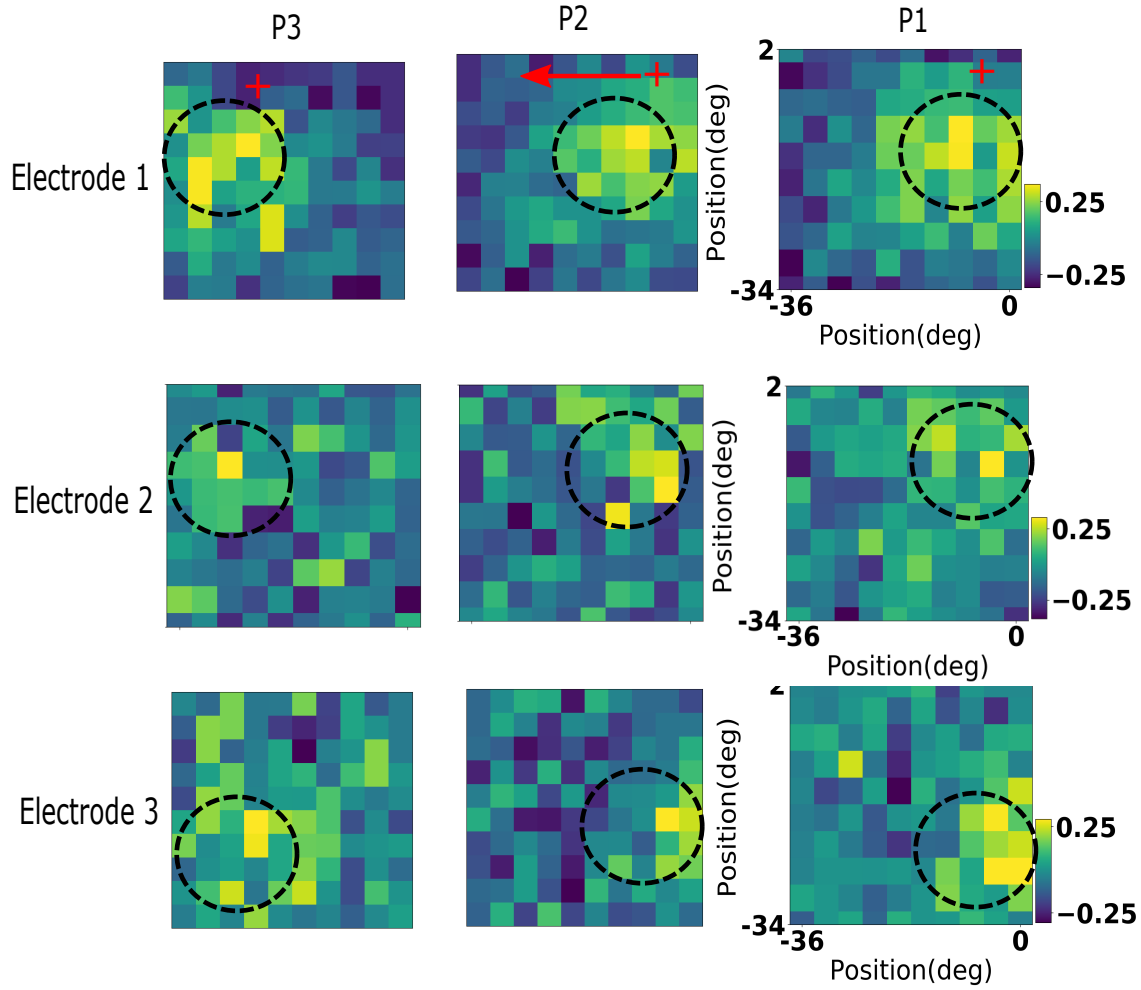
Figure 4.5 **Weight fields with respect to LFP responses.** Calculated weight values for each electrode, for localizing each probe position, have been illustrated in the location of visual stimuli for P1, P2 and P3, using LFP responses. The three selected electrodes, are sampled out of 96 for better visualization purposes.

Visual prostheses applications are working with weight fields to generate patterns. To investigate the mislocalization phenomenon in visual prostheses during the saccade, we analysed the transient shift in the weight field assigned to each probe position through a support vector machine (SVM). Also, we studied how the centre of the weight field (WF) changes relatively to the receptive field (RF) in pre, peri, and post saccade.

To investigate the mislocalization phenomenon on weight fields (WF), we examined the dynamics of future field (FF) and current field (CF) vectors. These vectors respectively correspond to the centre of weight field in the fixation point to the saccade target (FF), and, the vector which connects the centre of weight fields in the immediate of the saccade, to the saccade target. This investigation will help us to understand if we can capture the same behaviour in weight fields as the receptive field in the presence of eye movements.

In order to determine the relationship between receptive field and weight field centres for each electrode, we calculated the spatial distance between their centres. This is important since it shows the coding strategy (weight assignment) used by the decoder for localization. Foroushani *et al.* 2020 [11] showed that, for discriminating the positions of pair of a probes with a small separation, the centre of weight field will locate on the flank of the receptive field. On the other hand, for larger separations, weight field centres tend to locate close to the receptive field centre [11, 112]. However, in our problem, that is essentially localization, we are discriminating a position from both small and large separations. Therefore, we expect to see various distances between centres of weight fields and centre of receptive fields. In order to visualize it, for every electrode, we used histograms to present distribution of these distances, shown in figure 4.6.

Using MUA data, when the monkey has fixated his gaze, as for P1 and P3, see figure 4.6 sections *A* and *C*, there are many electrodes with small distance between WF and RF. This suggests that, most of the probes are located in the farther distances from a specific probe. This make sense because the number of more distant probes is higher than the number of less distant ones. However, in P2, see figure 4.6 section *B*, at the time of saccade, this pattern breaks which suggests that weights are not assigned well, leading to higher misclassification rate. For P2, we can observe that distances around the mean (25°) are dominant. This confirms the mislocalization phenomenon that happens just before the saccade [3]. Saccade preparation increases the distance between the weight field and the receptive field centres.

With LFP, similar behaviour occurs but it is less observable. To quantitatively, show this similarity, we fitted Gamma distribution to the histograms. Our results showed that the peak of distribution for P2 has been shifted to the right compare to P1 and P3.

Studying the dynamics of saccade vectors on weight fields show that, in the onset of the saccade, the vector between the centres of weight fields in perisaccadic to postsaccadic (remapping vector), has a shift in comparison to the vectors of presaccade to postsaccade (actual vector). In other words, by investigating weight fields mislocalization we can observe that the decoding ability will change as the modification or shift in the receptive field. To study the effect of mislocalization, we compared the magnitude of remapping and actual vectors. Also, the angle between the remapping and the actual vectors was calculated by equation 3.9. We performed t-test which determine if the remapping vector differed from the actual vector.

H0: difference between magnitudes of two vectors is zero, no difference between vectors.
H1: difference between magnitudes of two vectors is not zero, P2 has an effect.

In table 4.2 the P_{value} for the magnitude of two vectors has been illustrated. We used this P_{value} to show that perisaccadic to postsaccadic vector is not complying with the presaccadic to postsaccadic vector. Thus, we can conclude that mislocalization is happening in weight fields. For both MUA and LFP, the p_{value} of magnitude is less than 0.05 which shows a significant change from remapping vector to actual vector. Also, the values of the angle between the vectors indicate changes in them. Since the calculated angles represent values greater than zero, this means that the remapping and actual vectors has different direction.

P2 weights, that are SVM weights assigned to each electrode when mislocalization happens, can be used to imitate the process of localization for cortical prostheses applications. To obtain a stable pattern by inducing phosphenes during saccade in visual prostheses, we need

Table 4.2 $\boldsymbol{P_{value}}$ **for the magnitude of remapping and actual vectors**

Signal	P_{value}
Local Field Potential (LFP)	0.0046
Multiunit Activities (MUA)	0.0009
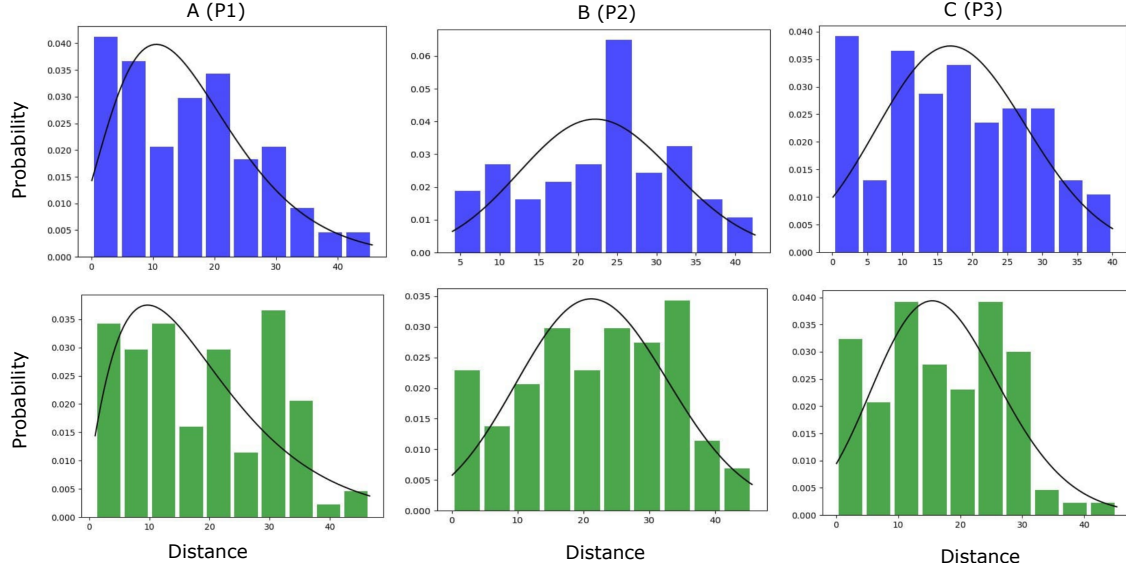
Figure 4.6 **Graphical representation of distribution of distances between centres of RF, WF.** Histogram of Euclidean distance between the centre of receptive fields and weight fields for all 96 electrodes with MUA (top - blue graphs) and LFP (bottom - green graphs) and fitted gamma distribution. (Left) P1, (Middle) P2, (Right) P3. Ten bins were considered for the histogram. In each graph, the x-axis shows Euclidean distance ranges (visual degree) and the y-axis represents the rate of electrode existence with specific x_{value}.

to be able to select electrodes in all steps of the saccade. For this purpose, our decoder provides weights that corresponds to the electrode's importance level for localizing each probe position on the grid during saccade, see equation 3.5. As it is shown in figures 4.11 and 4.12, each electrode in any state of a saccade can localize a specific probe. Besides, as extracted weights from our proposed decoder showed the same behaviour in presence of saccadic eye movements, we can anticipate that by using this technique in visual prostheses we can provide a stable percept which is comparable with the natural visual system.
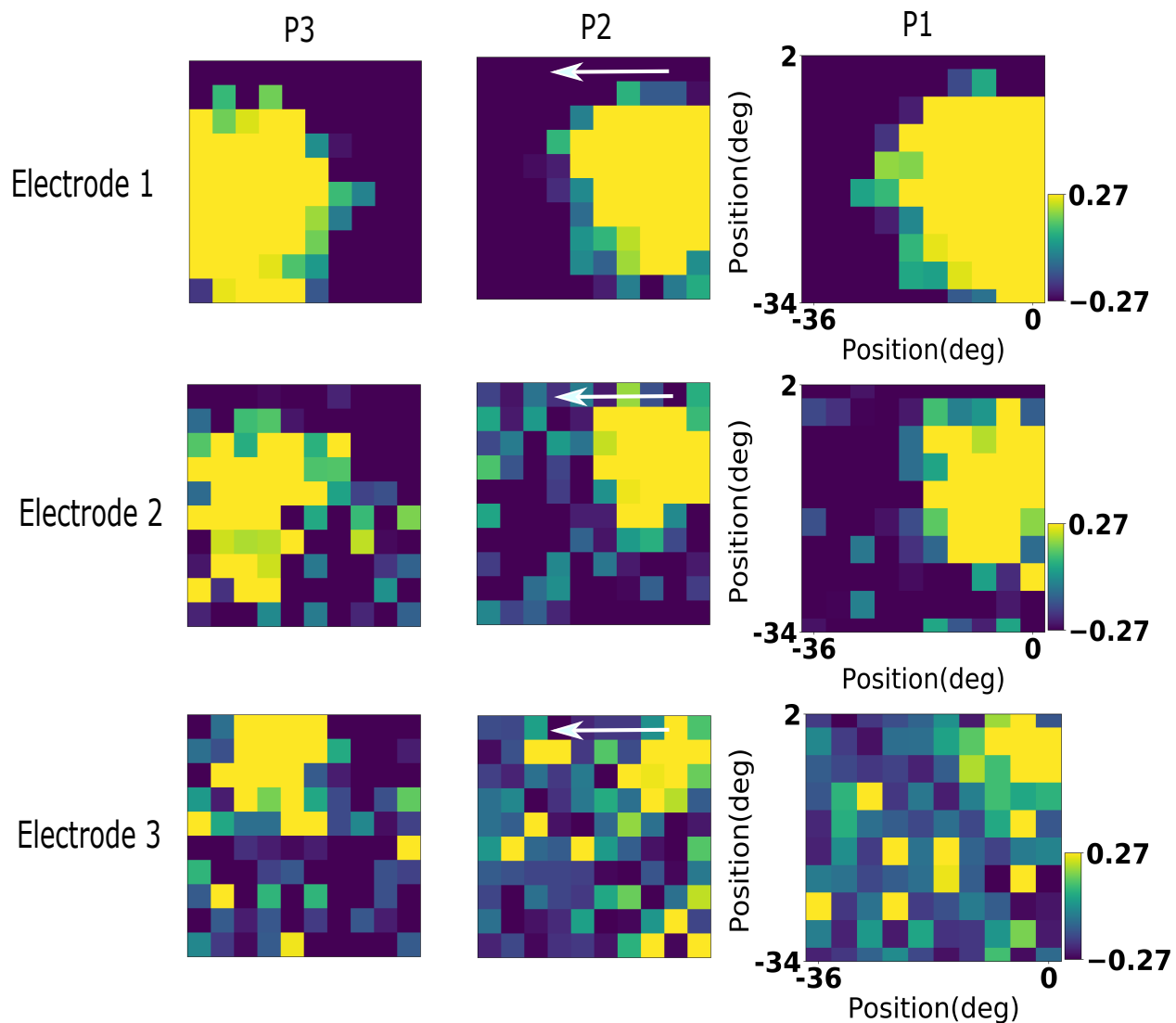
Figure 4.7 **Receptive field with respect to MUA responses.** Change in the position of an example neuron's receptive field with respect to the state of saccade. In state P2, the receptive field is shifted towards the saccade target (P3). The white arrow shows the change on receptive field in the state P2 towards the saccade target.
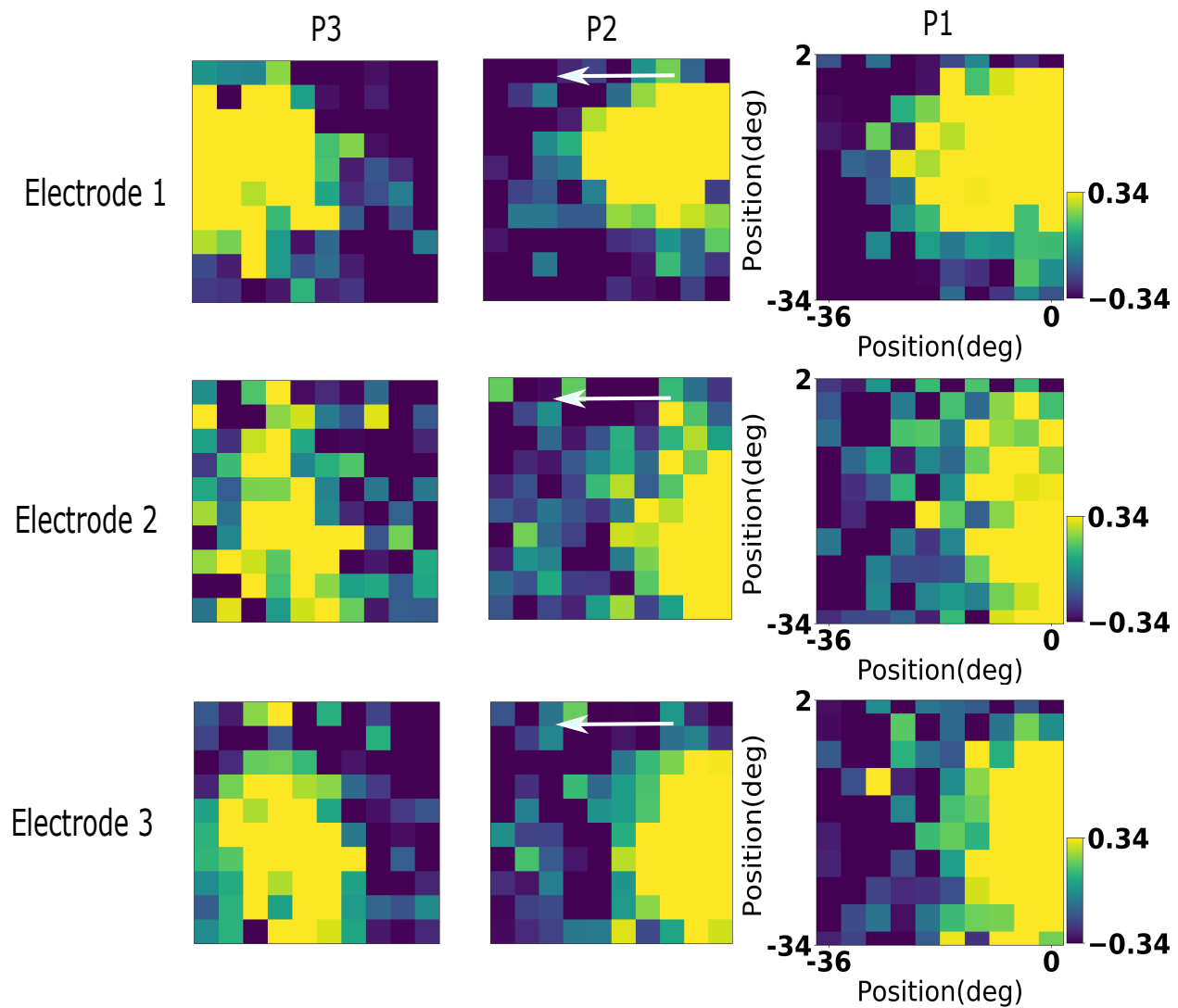
Figure 4.8 **Receptive field with respect to LFP responses.** Chang in the position of an example neuron's receptive field with respect to the state of saccade. In state P2, the receptive field is shifted towards the saccade target (P3). The white arrow shows the change on receptive field in the state P2 towards the saccade target.

Electrode 1   **Electrode 2**   **Electrode 3**

(-5.72, -17.14)   (-4.62, -12.35)   (-4.53, -2.08)

(-6.08,-15.39)   (-5.49,-10.05)   (-4.25,-2.70)

(-27.36, -18.41)   (-26.39, -12.34)   (-23.63, -3.08)
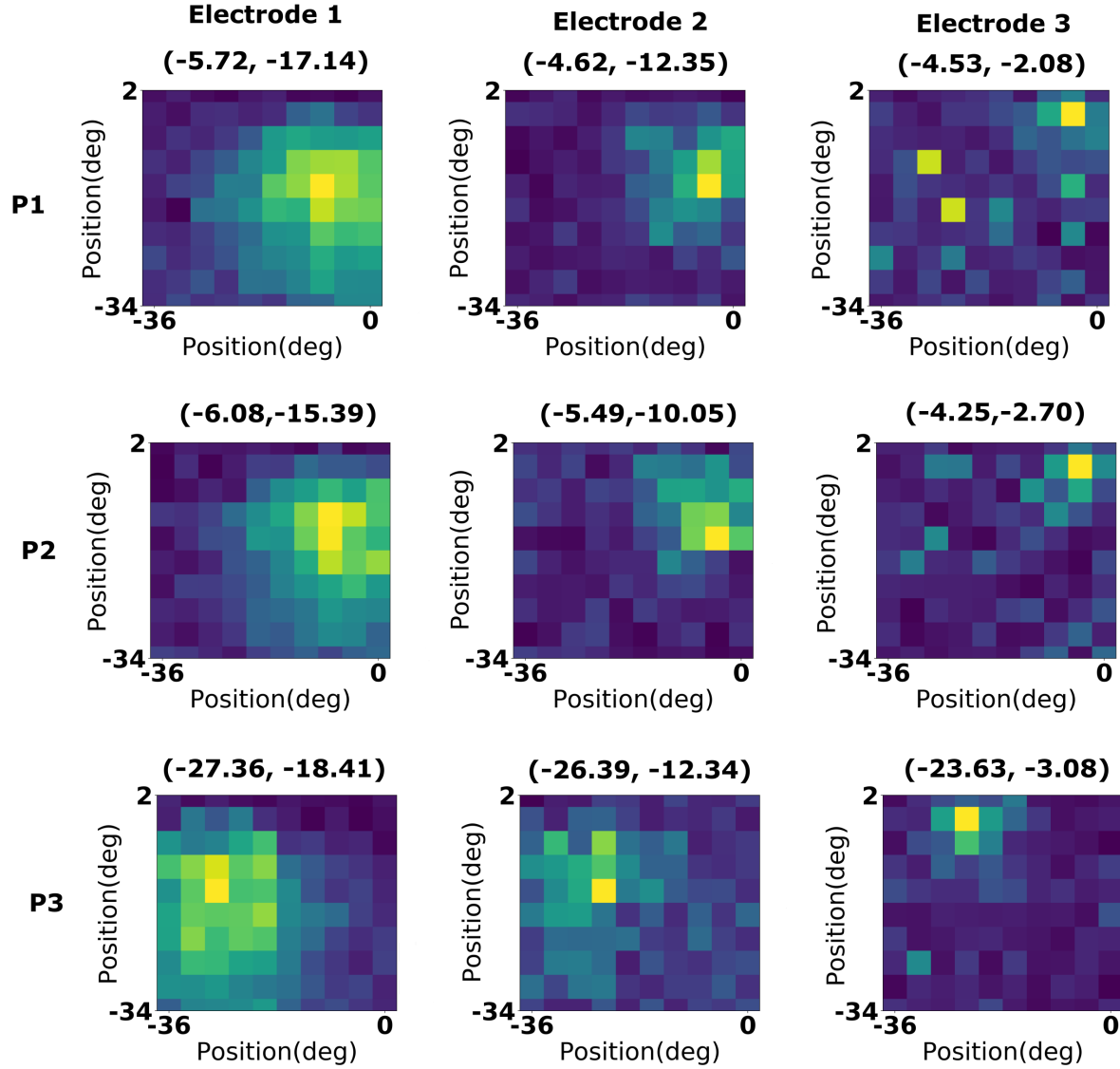
Figure 4.9 **Centre of weight fields concerning MUA responses.** In each step of the saccade, the centre of weight fields has been calculated in order to investigate mislocalization phenomena. For calculating the centre of weight fields we fitted a two-dimensional Gaussian model to them.
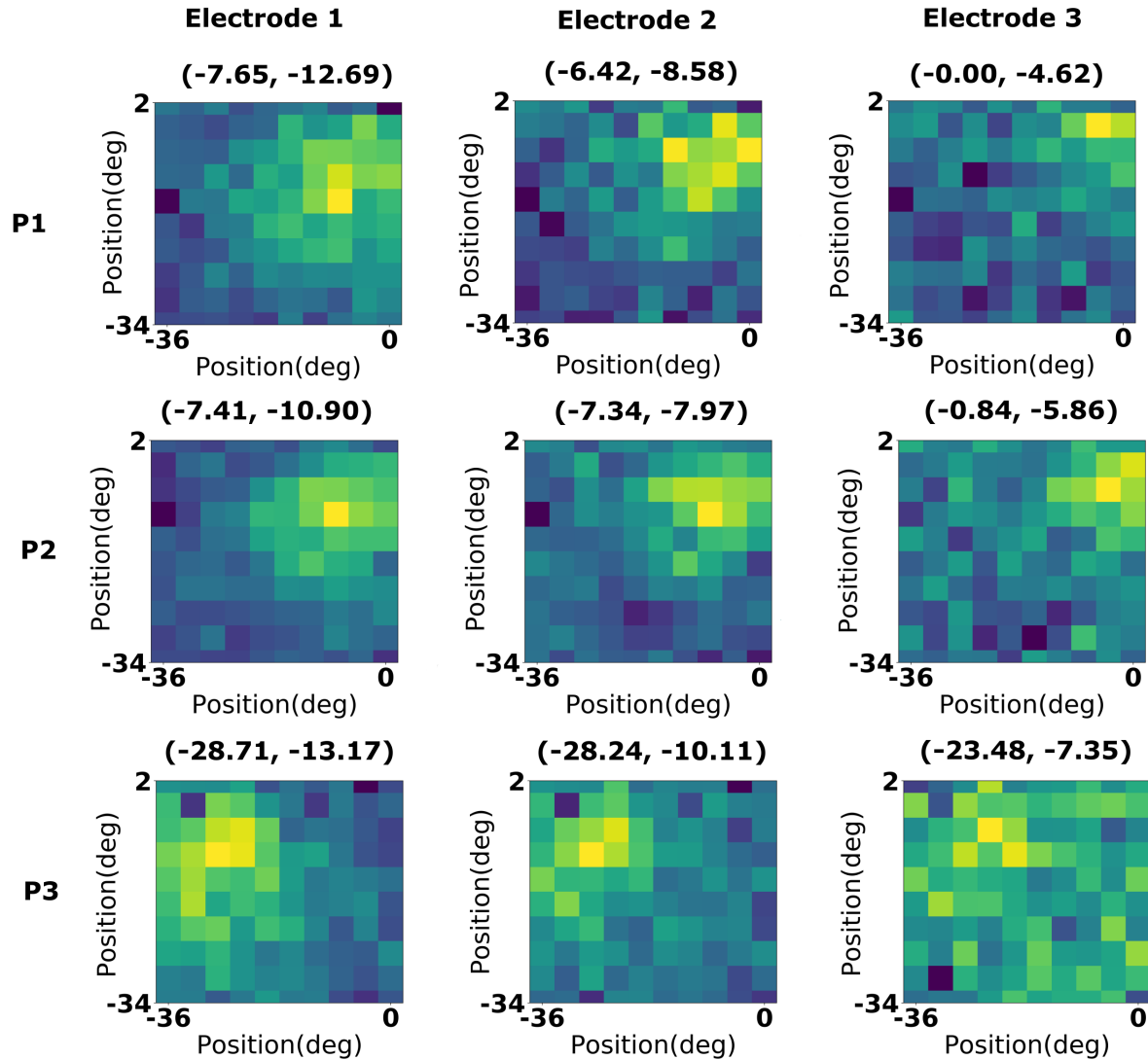
Figure 4.10 **Center of weight fields concerning LFP responses.** In each step of the saccade, the center of weight fields has been calculated in order to investigate mislocalization phenomena. For calculating the centre of weight fields we fitted a two-dimensional Gaussian model to them.
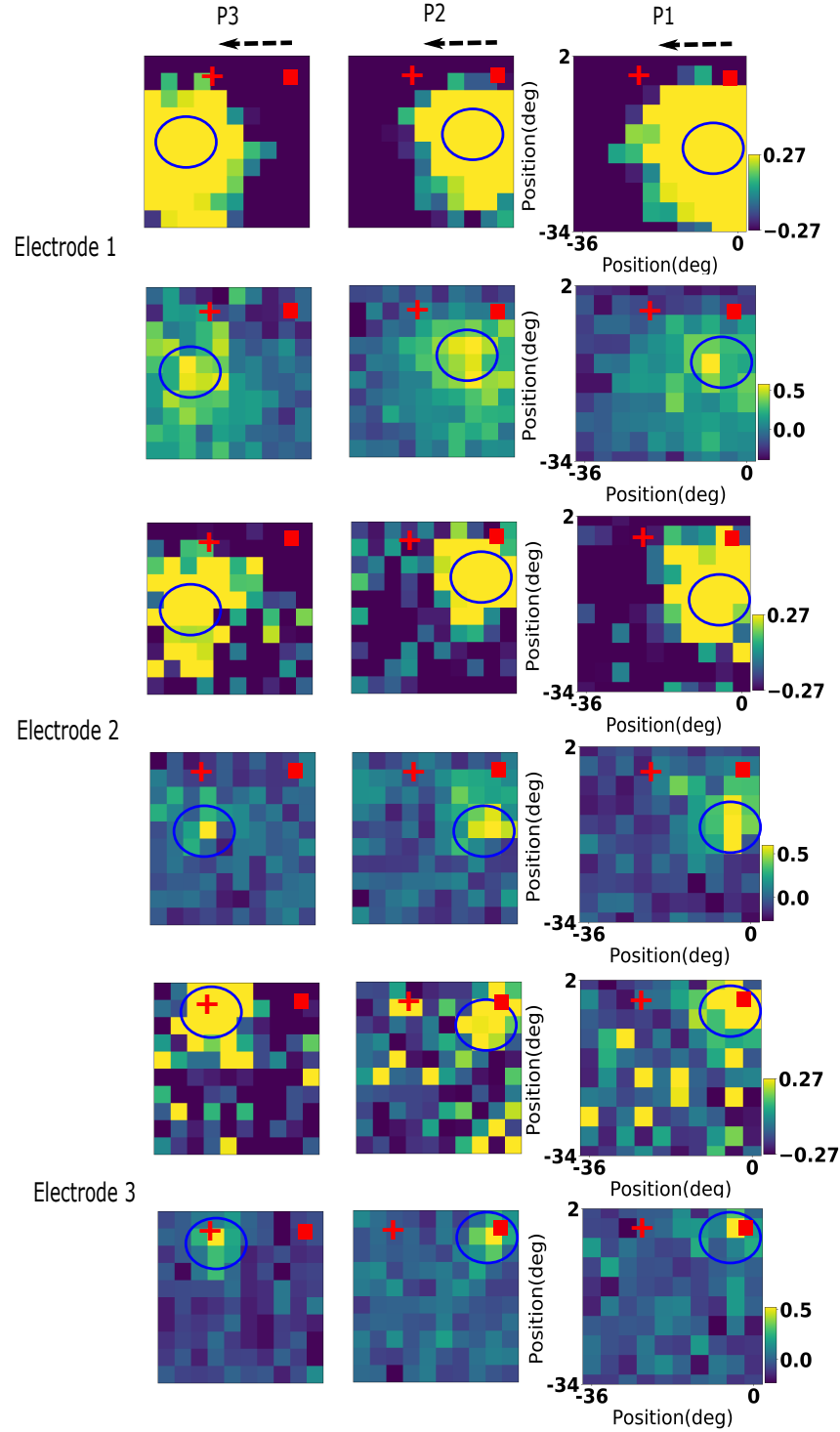
Figure 4.11 **The shift in centres of weight and receptive fields concerning MUA responses.** Shift in the localization capability of V4 before the saccade (P1), slightly before saccade but after the change in the location of the fixation point (P2), and after the saccade (P3). Blue circles are showing the centres of the weight and receptive fields. On the plots, we can see that the centre of the receptive field and weight field are corresponding to each other in all states of eye movements.
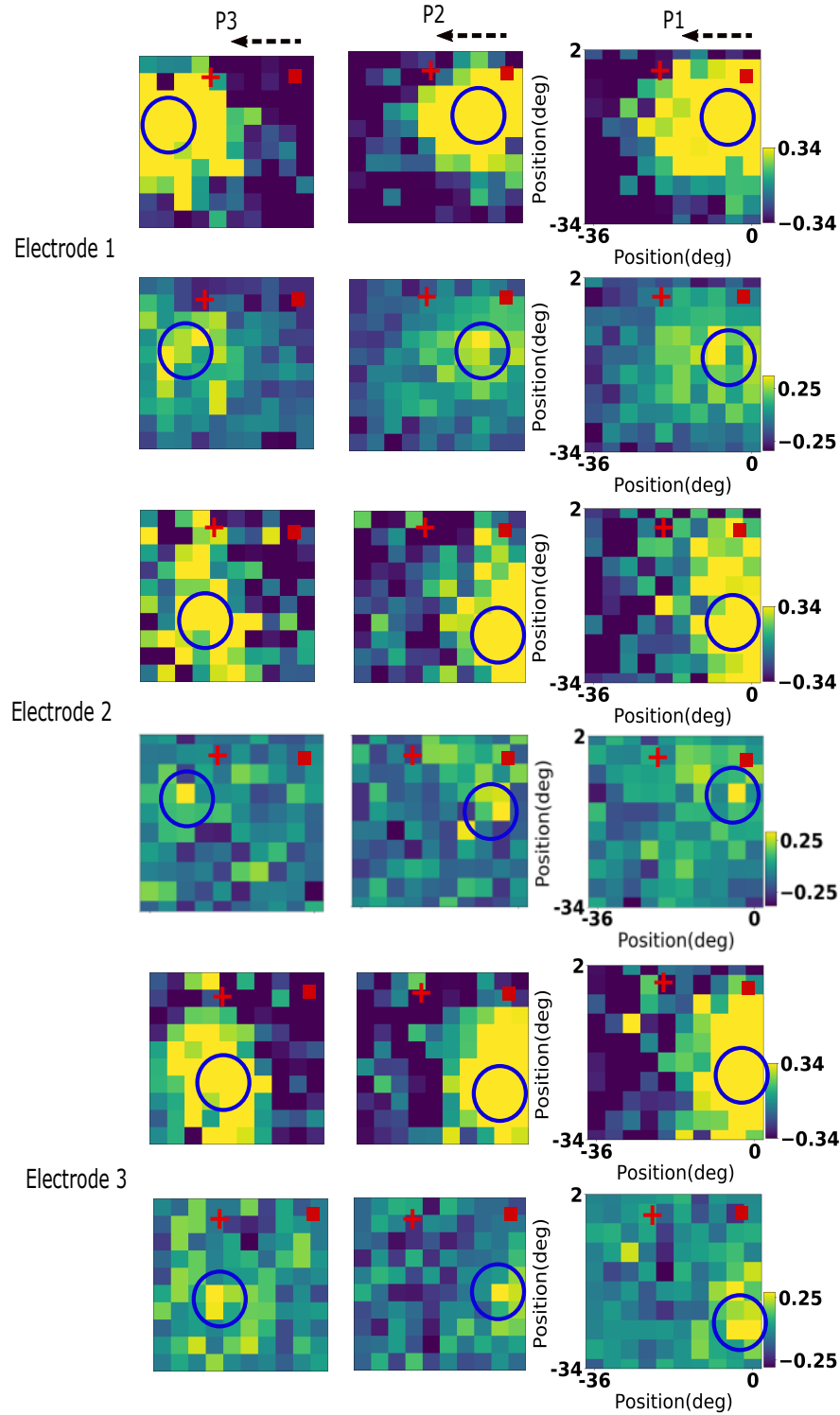
Figure 4.12 **The shift in centres of weight and receptive fields concerning LFP responses.** Shift in the localization capability of V4 before the saccade (P1), slightly before saccade but after the change in the location of the fixation point (P2), and after the saccade (P3). Blue circles are showing the centres of the weight and receptive fields. On the plots, we can see that the centre of the receptive field and weight field are corresponding to each other in all states of eye movements.

CHAPTER 5   DISCUSSION

We move our eyes to explore the world around us. These movements make changes in the positions of the objects in the retina. Despite that, the natural visual system provides us with a stable perception of the world around us without us realizing it. In other words, our brain compensates for this displacement. However, the perisaccadic perceptual space is distorted. Most of the previous studies in cortical visual prostheses were based on creating stimulating patterns when the eye is fixing on a position. In other words, such a system is providing a discrete image and fails to update the visual information with the eye movement. Spatial updating in artificial vision applications are essential in order to create a stable image for human with visual damage.

In this master project we quantitatively showed how much saccade preparation influences localization capability of V4. These results can help generating stable percepts using visual prosthetic devices. First, we proposed a decoder that was able to localize probe positions not only when eyes were fixating on a point, but also in the onset of saccade. The results of this study can be applied to visual prosthetic devices that require creating stable images. For this purpose, we used Multiunit Activity (MUA) and Local Field Potentials (LFPs) recorded data from visual cortex V4 in macaque monkey. We compared the performance of the decoder in fixation conditions versus saccade initialization condition. For this, we compared the extracted electrode weights from decoders in pre (P1), peri (P2), and post (P3) saccadic eye movement.

5.1   Summary of Works

Visual impairment can have devastating impacts on people's life. Fortunately, many studies have been on artificial vision. The visual prosthetic application's goal is to recover the vision function of people with visual impairment. However, one of the major problems in these devices is to generate stable and meaningful images from phosphene, cortical visual representation of light points, with the assist of applying electrical stimulation parameters to implanted electrodes. On the other hand, there are reports about the failure of these devices in updating visual information in the time of saccade. Saccade is one of the main eye movements we make to scan the world around us in order to have a stable image from the

visual scene. One of the prospective solutions for this failure in the prosthetic application is to inducing phosphenes at multiple positions stably by artificially creating the visual system mechanism called remapping. For this purpose, we need to understand how this visual remapping works and how saccadic eye movements affect the localization of each stimulus in the visual cortex.

This thesis interest was to propose a decoder for real visual prosthesis application with the ability to generate a stable percept not only in the fixation point but also in the onset of saccade by discriminating each probe position from the others. This gives important information to induce a phosphene in a specific location in the visual fields. In addition, we studied this phenomenon in both Multiunit Activity (MUA) and Local Field Potentials (LFPs). Using LFP responses for investigating probe localization for visual prostheses applications is important because, they are more stable and can be measured consistently for years after multi-electrode arrays have been implanted [11, 113]. Also, we showed that perisaccadic distortion can be traced to the electrode weights which were extracted from the implanted multielectrode array in visual cortex V4.

For this purpose, we studied the correspondant of changes in our proposed decoder weights with respect to the changes in the receptive field in presence of saccadic eye movements. Study of the decoding weights indicated that each electrode would precisely localize position located at its receptive field centre when we consider discrimination of a probe position from the others.

Besides, previous studies in prosthesis applications were focusing on discrimination between a pair of visual positions although in our study we considered probe localization by discriminating each probe from the rest of the probes on the grid. Overall, according to the obtained results, it can be concluded that, by using our proposed method, we can control the weights of the electrodes even during a saccade. Consequently, we can change them so that the image stays stable in visual applications during eye movements. In other words, we can rearrange the stimuli that are given to the electrodes for phosphene induction. By this method, we can expect to have the same behaviour as healthy visual system for scanning the world and generating stable percept.

5.1.1 Recommendations

What is important to remember is that decoders typically evaluate the evoked neural activity response. Response measurements are collected on the basis of certain hypotheses concerning the signal and the verification of the capacity of the response to discriminate. However, this can lead to bias in the outcome, since it requires assumptions about the response measures. An approach to address this obstacle is to use all temporal neural activity samples to train the decoder instead of a single response value. Although this is a more reliable approach, it requires more data and a more complex model, like a neural network (NN) or convolutional neural network (CNN), in order to calculate the decision boundary.

The generation of phosphonated perceptions is created by electrical current pulse stimulation in almost all cortical visual prostheses studies, regardless of whether an anticipated pattern of neural activity is developed. These activation waveforms add new neuronal behaviour to the brain that might not be interpreted by brain circuits and, as a result, intensive preparation sessions would be needed to identify these unnatural patterns of activity. Major work is therefore needed to invent stimulus techniques that can produce preformed neural activity patterns that correlate to meaningful perceptions.

5.2 Limitations

Limitations of this work are described below:

- Another mechanism use by the brain to provide image stability by decreasing neural responses around the time of saccade is called saccadic suppression. This mechanism besides remapping is essential for having stable percepts in visual application prostheses. In this work, we considered just mislocalization phenomenon during saccade for probe localization. However, having visual prostheses that are able to produce a stable world for people with a visual impairment also requires to have the same mechanisms as saccadic suppression.

- The proposed decoder needs more amount of recordings for each probe per session to have better precision with the lower level of overfitting. However, it would be difficult for monkeys to perform more than a specific number of trials per session.

– Despite the fact that LFP responses are more long-lasting and resistant than MUA, they have a lower spatial resolution which makes them less appropriate for implantation of electrodes in the peripheral and even parafoveal regions. Consequently, to achieve accurate precision for LFP, the electrodes have to be implanted in the foveal representation.

5.3 Future Research

In this work, we presented a coding strategy for localization purpose by discriminating each probe position from the rest of the probes in presence of saccadic eye movements, in order to create a stable percept in visual prostheses applications. However, still, further studies are required to create cortical visual prostheses that interface with the real visual system. Some of the possible future work is described in the following.

In visual prostheses applications, it is not easy to produce a particular pattern of neural activity by implementing a spatiotemporal microstimulation pattern, since neuron activation can be spread without any control. The activation pattern is influenced by numerous factors like the configuration of implanted neural circuits. The continuation of this project would also include the creation of a statistical model to approximate the pattern of microstimulation for a particular pattern of neural activity.

In this work, we use data based on the neural activities recorded during electrical stimulation, meaning that we stimulate a current anywhere on the grid. Since this current is an electrical signal, it cannot activate the desired point as expected. This means that the created neural activity is distributed, which needs to be taken into account in future researches. For this purpose, more details must be considered to convert this current into the desired pattern of activation for it can accurately localize the required position.

Besides, the results obtained in this study are based on the data acquired from presenting only one probe at a time. Future paradigms should be on a pair of probes. Therefore, in each trial, multiple stimuli should be presented at the same time.

REFERENCES

[1] R. Q. Quiroga and S. Panzeri, "Extracting information from neuronal populations: information theory and decoding approaches," *Nature Reviews Neuroscience*, vol. 10, no. 3, pp. 173–185, 2009.

[2] A. N. Foroushani, C. C. Pack, and M. Sawan, "Cortical visual prostheses: from microstimulation to functional percept," *Journal of neural engineering*, vol. 15, no. 2, p. 021005, 2018.

[3] S. Neupane, D. Guitton, and C. C. Pack, "Two distinct types of remapping in primate cortical area v4," *Nature communications*, vol. 7, no. 1, pp. 1–11, 2016.

[4] N. Paraskevoudi and J. S. Pezaris, "Eye movement compensation and spatial updating in visual prosthetics: mechanisms, limitations and future directions," *Frontiers in Systems Neuroscience*, vol. 12, p. 73, 2019.

[5] G. S. Brindley and W. S. Lewin, "The sensations produced by electrical stimulation of the visual cortex," *The Journal of Physiology*, vol. 196, no. 2, pp. 479–493, 1968.

[6] D. Burr, "Eye movements: keeping vision stable," *Current Biology*, vol. 14, no. 5, pp. R195–R197, 2004.

[7] L. M. Heiser and C. L. Colby, "Spatial updating in area lip is independent of saccade direction," *Journal of neurophysiology*, vol. 95, no. 5, pp. 2751–2767, 2006.

[8] T. P. Zanos, P. J. Mineault, D. Guitton, and C. C. Pack, "Mechanisms of saccadic suppression in primate cortical area v4," *Journal of Neuroscience*, vol. 36, no. 35, pp. 9227–9239, 2016.

[9] M. A. Sommer and R. H. Wurtz, "Brain circuits for the internal monitoring of movements," *Annu. Rev. Neurosci.*, vol. 31, pp. 317–338, 2008.

[10] C. Colby, M. Goldberg *et al.*, "The updating of the representation of visual space in parietal cortex by intended eye movements," *Science*, vol. 255, no. 5040, pp. 90–92, 1992.

[11] A. N. Foroushani, S. Neupane, P. D. H. Pastor, C. C. Pack, and M. Sawan, "Spatial resolution of local field potential signals in macaque v4," *arXiv preprint arXiv:1911.07388*, 2019.

[12] M. A. Sommer and R. H. Wurtz, "Influence of the thalamus on spatial visual processing in frontal cortex," *Nature*, vol. 444, no. 7117, pp. 374–377, 2006.

[13] L. N. Ayton, N. Barnes, G. Dagnelie, T. Fujikado, G. Goetz, R. Hornig, B. W. Jones, M. M. Muqit, D. L. Rathbun, K. Stingl *et al.*, "An update on retinal prostheses," *Clinical Neurophysiology*, vol. 131, no. 6, pp. 1383–1398, 2020.

[14] S. Shim, K. Seo, and S. J. Kim, "A preliminary implementation of an active intraocular prosthesis as a new image acquisition device for a cortical visual prosthesis." *Journal of Artificial Organs: the Official Journal of the Japanese Society for Artificial Organs*, 2020.

[15] B. Krekelberg, M. Kubischik, K.-P. Hoffmann, and F. Bremmer, "Neural correlates of visual localization and perisaccadic mislocalization," *Neuron*, vol. 37, no. 3, pp. 537–545, 2003.

[16] W. H. Dobelle, "Artificial vision for the blind by connecting a television camera to the visual cortex," *ASAIO journal*, vol. 46, no. 1, pp. 3–9, 2000.

[17] L. B. Merabet, J. F. Rizzo, A. Amedi, D. C. Somers, and A. Pascual-Leone, "What blindness can tell us about seeing again: merging neuroplasticity and neuroprostheses," *Nature Reviews Neuroscience*, vol. 6, no. 1, pp. 71–77, 2005.

[18] W. H. Dobelle, M. G. Mladejovsky, and J. Girvin, "Artificial vision for the blind: electrical stimulation of visual cortex offers hope for a functional prosthesis," *Science*, vol. 183, no. 4123, pp. 440–444, 1974.

[19] E. Schmidt, M. Bak, F. Hambrecht, C. Kufta, D. O'rourke, and P. Vallabhanath, "Feasibility of a visual prosthesis for the blind based on intracortical micro stimulation of the visual cortex," *Brain*, vol. 119, no. 2, pp. 507–522, 1996.

[20] W. Dobelle and M. Mladejovsky, "Phosphenes produced by electrical stimulation of human occipital cortex, and their application to the development of a prosthesis for the blind," *The Journal of physiology*, vol. 243, no. 2, pp. 553–576, 1974.

[21] K. Cha, K. Horch, and R. A. Normann, "Simulation of a phosphene-based visual field: visual acuity in a pixelized vision system," *Annals of Biomedical Engineering*, vol. 20, no. 4, pp. 439–449, 1992.

[22] E. J. Tehovnik, "Electrical stimulation of neural tissue to evoke behavioral responses," *Journal of neuroscience methods*, vol. 65, no. 1, pp. 1–17, 1996.

[23] R. T. Born and D. C. Bradley, "Structure and function of visual area mt," *Annu. Rev. Neurosci.*, vol. 28, pp. 157–189, 2005.

[24] K. Britten, "The middle temporal area: Motion processing and the link to perception," *The visual neurosciences*, 2003.

[25] P. Lennie, "Single units and visual cortical organization," *Perception*, vol. 27, no. 8, pp. 889–935, 1998.

[26] P. J. Mineault, T. P. Zanos, and C. C. Pack, "Local field potentials reflect multiple spatial scales in v4," *Frontiers in computational neuroscience*, vol. 7, p. 21, 2013.

[27] R. Gattass, A. Sousa, and C. Gross, "Visuotopic organization and extent of v3 and v4 of the macaque," *Journal of Neuroscience*, vol. 8, no. 6, pp. 1831–1845, 1988.

[28] X. Yue, I. S. Pourladian, R. B. Tootell, and L. G. Ungerleider, "Curvature-processing network in macaque visual cortex," *Proceedings of the National Academy of Sciences*, vol. 111, no. 33, pp. E3467–E3475, 2014.

[29] A. Pasupathy and C. E. Connor, "Responses to contour features in macaque area v4," *Journal of neurophysiology*, vol. 82, no. 5, pp. 2490–2502, 1999.

[30] D. C. Bradley, P. R. Troyk, J. A. Berg, M. Bak, S. Cogan, R. Erickson, C. Kufta, M. Mascaro, D. McCreery, E. M. Schmidt *et al.*, "Visuotopic mapping through a multichannel stimulating implant in primate v1," *Journal of neurophysiology*, vol. 93, no. 3, pp. 1659–1670, 2005.

[31] E. J. Tehovnik and W. M. Slocum, "Microstimulation of macaque v1 disrupts target selection: effects of stimulation polarity," *Experimental brain research*, vol. 148, no. 2, pp. 233–237, 2003.

[32] E. J. Tehovnik, W. M. Slocum, and P. H. Schiller, "Differential effects of laminar stimulation of v1 cortex on target selection by macaque monkeys," *European Journal of Neuroscience*, vol. 16, no. 4, pp. 751–760, 2002.

[33] H. K. HARTLINE, "The neural mechanisms of vision h. keffer hartline," *Studies on Excitation and Inhibition in the Retina: A Collection of Papers from the Laboratories of H. Keffer Hartline*, p. 195, 1974.

[34] J. Churan, D. Guitton, and C. C. Pack, "Context dependence of receptive field remapping in superior colliculus," *Journal of neurophysiology*, vol. 106, no. 4, pp. 1862–1874, 2011.

[35] K. Nakamura and C. L. Colby, "Updating of the visual representation in monkey striate and extrastriate cortex during saccades," *Proceedings of the National Academy of Sciences*, vol. 99, no. 6, pp. 4026–4031, 2002.

[36] A. S. Tolias, T. Moore, S. M. Smirnakis, E. J. Tehovnik, A. G. Siapas, and P. H. Schiller, "Eye movements modulate visual receptive fields of v4 neurons," *Neuron*, vol. 29, no. 3, pp. 757–767, 2001.

[37] M. Zirnsak, N. A. Steinmetz, B. Noudoost, K. Z. Xu, and T. Moore, "Visual space is compressed in prefrontal cortex before eye movements," *Nature*, vol. 507, no. 7493, pp. 504–507, 2014.

[38] M. E. Goldberg and C. J. Bruce, "Primate frontal eye fields. iii. maintenance of a spatially accurate saccade signal," *Journal of neurophysiology*, vol. 64, no. 2, pp. 489–508, 1990.

[39] R. H. Wurtz and C. W. Mohler, "Enhancement of visual responses in monkey striate cortex and frontal eye fields," *Journal of neurophysiology*, vol. 39, no. 4, pp. 766–772, 1976.

[40] W. Wichmann and W. Müller-Forell, "Anatomy of the visual system," *European journal of radiology*, vol. 49, no. 1, pp. 8–30, 2004.

[41] L. A. Remington and D. Goodwin, *Clinical anatomy of the visual system E-Book.* Elsevier Health Sciences, 2011.

[42] K. Cherry, "What is self-efficacy? about. com psychology," 2014.

[43] S. R. y Cajal, "Visual system," *Eye*, vol. 2, p. 1.

[44] D. H. Hubel and T. N. Wiesel, "Ferrier lecture-functional architecture of macaque monkey visual cortex," *Proceedings of the Royal Society of London. Series B. Biological Sciences*, vol. 198, no. 1130, pp. 1–59, 1977.

[45] R. C. Reid and J.-M. Alonso, "Specificity of monosynaptic connections from thalamus to visual cortex," *Nature*, vol. 378, no. 6554, pp. 281–284, 1995.

[46] G. E. Schneider, "Two visual systems." *Science*, 1969.

[47] C. B. Trevarthen, "Two mechanisms of vision in primates," *Psychologische Forschung*, vol. 31, no. 4, pp. 299–337, 1968.

[48] M. Mishkin, M. E. Lewis, and L. G. Ungerleider, "Equivalence of parieto-preoccipital subareas for visuospatial ability in monkeys," *Behavioural brain research*, vol. 6, no. 1, pp. 41–55, 1982.

[49] T. Schenk and R. D. McIntosh, "Do we have independent visual streams for perception and action?" *Cognitive Neuroscience*, vol. 1, no. 1, pp. 52–62, 2010.

[50] M. A. Goodale, D. Pelisson, and C. Prablanc, "Large adjustments in visually guided reaching do not depend on vision of the hand or perception of target displacement," *Nature*, vol. 320, no. 6064, pp. 748–750, 1986.

[51] D. Milner and M. Goodale, *The visual brain in action.* OUP Oxford, 2006, vol. 27.

[52] T. Huff, N. Mahabadi, and P. Tadi, "Neuroanatomy, visual cortex," in *StatPearls [Internet].* StatPearls Publishing, 2019.

[53] A. Tran, M. W. MacLean, V. Hadid, L. Lazzouni, D. K. Nguyen, J. Tremblay, M. Dehaes, and F. Lepore, "Neuronal mechanisms of motion detection underlying blindsight assessed by functional magnetic resonance imaging (fmri)," *Neuropsychologia*, vol. 128, pp. 187–197, 2019.

[54] D. H. Hubel and T. N. Wiesel, "Laminar and columnar distribution of geniculo-cortical fibers in the macaque monkey," *Journal of Comparative Neurology*, vol. 146, no. 4, pp. 421–450, 1972.

[55] L. Zhaoping and Z. Li, *Understanding vision: theory, models, and data.* Oxford University Press, USA, 2014.

[56] K. Torab, T. Davis, D. Warren, P. House, R. Normann, and B. Greger, "Multiple factors may influence the performance of a visual prosthesis based on intracortical microstimulation: nonhuman primate behavioural experimentation," *Journal of neural engineering*, vol. 8, no. 3, p. 035001, 2011.

[57] C. J. McAdams and J. H. Maunsell, "Effects of attention on orientation-tuning functions of single neurons in macaque cortical area v4," *Journal of Neuroscience*, vol. 19, no. 1, pp. 431–441, 1999.

[58] A. W. Bitar, M. M. Mansour, and A. Chehab, "Algorithmic optimizations in the hmax model targeted for efficient object recognition," pp. 374–395, 2015.

[59] D. K. Murphey, J. H. Maunsell, M. S. Beauchamp, and D. Yoshor, "Perceiving electrical stimulation of identified human visual areas," *Proceedings of the National Academy of Sciences*, vol. 106, no. 13, pp. 5389–5393, 2009.

[60] G. A. Orban, "Higher order visual processing in macaque extrastriate cortex," *Physiological reviews*, 2008.

[61] S.-R. Afraz, R. Kiani, and H. Esteky, "Microstimulation of inferotemporal cortex influences face categorization," *Nature*, vol. 442, no. 7103, pp. 692–695, 2006.

[62] T. Yang and J. H. Maunsell, "The effect of perceptual learning on neuronal responses in monkey visual area v4," *Journal of Neuroscience*, vol. 24, no. 7, pp. 1617–1626, 2004.

[63] C. J. Duffy, "Mst neurons respond to optic flow and translational movement," *Journal of neurophysiology*, vol. 80, no. 4, pp. 1816–1827, 1998.

[64] Y. Gu, G. C. DeAngelis, and D. E. Angelaki, "Causal links between dorsal medial superior temporal area neurons and multisensory heading perception," *Journal of Neuroscience*, vol. 32, no. 7, pp. 2299–2313, 2012.

[65] K. Tsunoda, Y. Yamane, M. Nishizaki, and M. Tanifuji, "Complex objects are represented in macaque inferotemporal cortex by the combination of feature columns," *Nature neuroscience*, vol. 4, no. 8, pp. 832–838, 2001.

[66] B. Fischer and R. Boch, "Enhanced activation of neurons in prelunate cortex before visually guided saccades of trained rhesus monkeys," *Experimental Brain Research*, vol. 44, no. 2, pp. 129–137, 1981.

[67] P. Cavanagh, A. R. Hunt, A. Afraz, and M. Rolfs, "Visual stability based on remapping of attention pointers," *Trends in cognitive sciences*, vol. 14, no. 4, pp. 147–153, 2010.

[68] P. M. Lewis, H. M. Ackland, A. J. Lowery, and J. V. Rosenfeld, "Restoration of vision in blind individuals using bionic devices: a review with a focus on cortical visual prostheses," *Brain research*, vol. 1595, pp. 51–73, 2015.

[69] J. Ross, M. C. Morrone, M. E. Goldberg, and D. C. Burr, "Changes in visual perception at the time of saccades," *Trends in neurosciences*, vol. 24, no. 2, pp. 113–121, 2001.

[70] D. J. Felleman and D. C. Van Essen, "Distributed hierarchical processing in the primate cerebral cortex," in *Cereb cortex*. Citeseer, 1991.

[71] P. Troyk, M. Bak, J. Berg, D. Bradley, S. Cogan, R. Erickson, C. Kufta, D. McCreery, E. Schmidt, and V. Towle, "A model for intracortical visual prosthesis research," *Artificial organs*, vol. 27, no. 11, pp. 1005–1015, 2003.

[72] M. Bak, J. Girvin, F. Hambrecht, C. Kufta, G. Loeb, and E. Schmidt, "Visual sensations produced by intracortical microstimulation of the human occipital cortex," *Medical and Biological Engineering and Computing*, vol. 28, no. 3, pp. 257–259, 1990.

[73] T. Davis, R. Parker, P. House, E. Bagley, S. Wendelken, R. Normann, and B. Greger, "Spatial and temporal characteristics of v1 microstimulation during chronic implantation of a microelectrode array in a behaving macaque," *Journal of neural engineering*, vol. 9, no. 6, p. 065003, 2012.

[74] Z. M. Hafed, K. Stingl, K.-U. Bartz-Schmidt, F. Gekeler, and E. Zrenner, "Oculomotor behavior of blind patients seeing with a subretinal visual implant," *Vision research*, vol. 118, pp. 119–131, 2016.

[75] J. S. Pezaris and R. C. Reid, "Simulations of electrode placement for a thalamic visual prosthesis," *IEEE Transactions on Biomedical Engineering*, vol. 56, no. 1, pp. 172–178, 2008.

[76] S. Klauke, M. Goertz, S. Rein, D. Hoehl, U. Thomas, R. Eckhorn, F. Bremmer, and T. Wachtler, "Stimulation with a wireless intraocular epiretinal implant elicits visual percepts in blind humans," *Investigative ophthalmology & visual science*, vol. 52, no. 1, pp. 449–455, 2011.

[77] T. Fujikado, M. Kamei, H. Sakaguchi, H. Kanda, T. Morimoto, Y. Ikuno, K. Nishida, H. Kishima, T. Maruo, K. Konoma *et al.*, "Testing of semichronically implanted retinal prosthesis by suprachoroidal-transretinal stimulation in patients with retinitis pigmentosa," *Investigative ophthalmology & visual science*, vol. 52, no. 7, pp. 4726–4733, 2011.

[78] K. Stingl, K. Bartz-Schmidt, D. Besch, A. Braun, A. Bruckmann, F. Gekeler, U. Greppmaier, and S. Hipp, "Ho rtdo rfer g, kernstock c, koitschev a, kusnyerik a, sachs h, schatz a, stingl kt, peters t, wilhelm b, zrenner e. 2013. artificial vision with wirelessly powered subretinal electronic implant alpha-ims," *Proceedings of the Royal Society B: Biological Sciences*, vol. 280, p. 20130077.

[79] F. Richlan, B. Gagl, S. Schuster, S. Hawelka, J. Humenberger, and F. Hutzler, "A new high-speed visual stimulation method for gaze-contingent eye movement and brain activity studies," *Frontiers in systems neuroscience*, vol. 7, p. 24, 2013.

[80] W. M. Slocum and E. J. Tehovnik, "Microstimulation of v1 input layers disrupts the selection and detection of visual targets by monkeys," *European Journal of Neuroscience*, vol. 20, no. 6, pp. 1674–1680, 2004.

[81] A. Caspi, A. Roy, J. D. Dorn, and R. J. Greenberg, "Retinotopic to spatiotopic mapping in blind patients implanted with the argus ii retinal prosthesis," *Investigative Ophthalmology & Visual Science*, vol. 58, no. 1, pp. 119–127, 2017.

[82] M. A. Nicolelis, D. Dimitrov, J. M. Carmena, R. Crist, G. Lehew, J. D. Kralik, and S. P. Wise, "Chronic, multisite, multielectrode recordings in macaque monkeys," *Proceedings of the National Academy of Sciences*, vol. 100, no. 19, pp. 11 041–11 046, 2003.

[83] R. Crist and M. Lebedev, "Multielectrode recording in behaving monkeys," in *Methods for Neural Ensemble Recordings. 2nd edition.* CRC Press/Taylor & Francis, 2008.

[84] M. A. Nicolelis, *Methods for neural ensemble recordings.* CRC press, 2007.

[85] J. Hu, X. M. Song, Q. Wang, and A. W. Roe, "Curvature domains in v4 of macaque monkey," *bioRxiv*, 2020.

[86] D. T. Gray and C. A. Barnes, "Experiments in macaque monkeys provide critical insights into age-associated changes in cognitive and sensory function," *Proceedings of the National Academy of Sciences*, vol. 116, no. 52, pp. 26 247–26 254, 2019.

[87] R. Passingham, "How good is the macaque monkey model of the human brain?" *Current opinion in neurobiology*, vol. 19, no. 1, pp. 6–11, 2009.

[88] R. C. Dodge, "Ts (1901)," *The angle velocity of eye movements. Psychol. Rev*, vol. 8, pp. 145–57.

[89] J. O'keefe and L. Nadel, *The hippocampus as a cognitive map.* Oxford: Clarendon Press, 1978.

[90] H. Hemholtz, "Helmholtz's treatise on physiological optics, 3rd german ed," *Southall JPC, trans. Rochester, NY: Optical Society of America*, 1925.

[91] R. J. Leigh and D. S. Zee, *The neurology of eye movements.* OUP USA, 2015.

[92] H. Deubel, W. X. Schneider, and B. Bridgeman, "Postsaccadic target blanking prevents saccadic suppression of image displacement," *Vision research*, vol. 36, no. 7, pp. 985–996, 1996.

[93] L. Matin and D. G. Pearce, "Visual perception of direction for stimuli flashed during voluntary saccadic eye movements," *Science*, vol. 148, no. 3676, pp. 1485–1488, 1965.

[94] N. Bischof and E. Kramer, "Untersuchungen und überlegungen zur richtungswahrnehmung bei willkürlichen sakkadischen augenbewegungen," *Psychologische Forschung*, vol. 32, no. 3, pp. 185–218, 1968.

[95] P. Dassonville, J. Schlag, and M. Schlag-Rey, "Oculomotor localization relies on a damped representation of saccadic eye displacement in human and nonhuman primates," *Visual neuroscience*, vol. 9, no. 3-4, pp. 261–269, 1992.

[96] M. C. Morrone, J. Ross, and D. C. Burr, "Apparent position of visual targets during real and simulated saccadic eye movements," *Journal of Neuroscience*, vol. 17, no. 20, pp. 7941–7953, 1997.

[97] M. M. Umeno and M. E. Goldberg, "Spatial processing in the monkey frontal eye field. i. predictive visual responses," *Journal of neurophysiology*, vol. 78, no. 3, pp. 1373–1383, 1997.

[98] M. Kaiser and M. Lappe, "Perisaccadic mislocalization orthogonal to saccade direction," *Neuron*, vol. 41, no. 2, pp. 293–300, 2004.

[99] C. W. Mohler and R. H. Wurtz, "Organization of monkey superior colliculus: intermediate layer cells discharging before eye movements," *Journal of neurophysiology*, vol. 39, no. 4, pp. 722–744, 1976.

[100] L. E. Mays and D. L. Sparks, "Dissociation of visual and saccade-related responses in superior colliculus neurons," *journal of Neurophysiology*, vol. 43, no. 1, pp. 207–232, 1980.

[101] E. P. Merriam, C. R. Genovese, and C. L. Colby, "Remapping in human visual cortex," *Journal of neurophysiology*, vol. 97, no. 2, pp. 1738–1755, 2007.

[102] L. D. Sun and M. E. Goldberg, "Corollary discharge and oculomotor proprioception: cortical mechanisms for spatially accurate vision," *Annual review of vision science*, vol. 2, pp. 61–84, 2016.

[103] T. Klucken, S. Kagerer, J. Schweckendiek, K. Tabbert, D. Vaitl, and R. Stark, "Neural, electrodermal and behavioral response patterns in contingency aware and unaware subjects during a picture–picture conditioning paradigm," *Neuroscience*, vol. 158, no. 2, pp. 721–731, 2009.

[104] T. Moore, A. S. Tolias, and P. H. Schiller, "Visual representations during saccadic eye movements," *Proceedings of the National Academy of Sciences*, vol. 95, no. 15, pp. 8981–8984, 1998.

[105] C. E. Connor, J. L. Gallant, D. C. Preddie, and D. C. Van Essen, "Responses in area v4 depend on the spatial relationship between stimulus and attention," *Journal of neurophysiology*, vol. 75, no. 3, pp. 1306–1308, 1996.

[106] T. P. Zanos, P. J. Mineault, K. T. Nasiotis, D. Guitton, and C. C. Pack, "A sensorimotor role for traveling waves in primate visual cortex," *Neuron*, vol. 85, no. 3, pp. 615–627, 2015.

[107] G. M. Ghose and D. Y. Ts' O, "Form processing modules in primate area v4," *Journal of Neurophysiology*, vol. 77, no. 4, pp. 2191–2196, 1997.

[108] T. P. Zanos, P. J. Mineault, and C. C. Pack, "Removal of spurious correlations between spikes and local field potentials," *Journal of neurophysiology*, vol. 105, no. 1, pp. 474–486, 2010.

[109] R. Q. Quiroga, Z. Nadasdy, and Y. Ben-Shaul, "Unsupervised spike detection and sorting with wavelets and superparamagnetic clustering," *Neural computation*, vol. 16, no. 8, pp. 1661–1687, 2004.

[110] A. D. Huberman, M. Manu, S. M. Koch, M. W. Susman, A. B. Lutz, E. M. Ullian, S. A. Baccus, and B. A. Barres, "Architecture and activity-mediated refinement of axonal projections from a mosaic of genetically identified retinal ganglion cells," *Neuron*, vol. 59, no. 3, pp. 425–438, 2008.

[111] H. Honda, "The time courses of visual mislocalization and of extraretinal eye position signals at the time of vertical saccades," *Vision research*, vol. 31, no. 11, pp. 1915–1921, 1991.

[112] D. A. Butts and M. S. Goldman, "Tuning curves, neuronal variability, and sensory coding," *PLoS Biol*, vol. 4, no. 4, p. e92, 2006.

[113] B. Pesaran, J. S. Pezaris, M. Sahani, P. P. Mitra, and R. A. Andersen, "Temporal structure in neuronal activity during working memory in macaque parietal cortex," *Nature neuroscience*, vol. 5, no. 8, pp. 805–811, 2002.